Studies of the Energy Dependence of Diboson Polarization Fractions and the Radiation Amplitude Zero Effect in WZ Production with the ATLAS Detector

Prachi Arvind Atmasiddha (University of Pennsylvania)

On behalf of the ATLAS Collaboration

DPF-PHENO 2024

15th May 2024

Why do we want to measure diboson polarization?

Massive gauge bosons gain an extra longitudinal degree of freedom via Higgs Mechanism along with the transverse ones.

Polarization: alignment of a particle's spin with its momentum. This is quantified by helicity (h).

- For transverse polarization (T), $h = \pm 1$. Like the two polarizations observed in photon (which is massless)
- **For the longitudinal polarization *(0 or L)*, $h = 0$. Additional degree of freedom present for massive gauge bosons.**

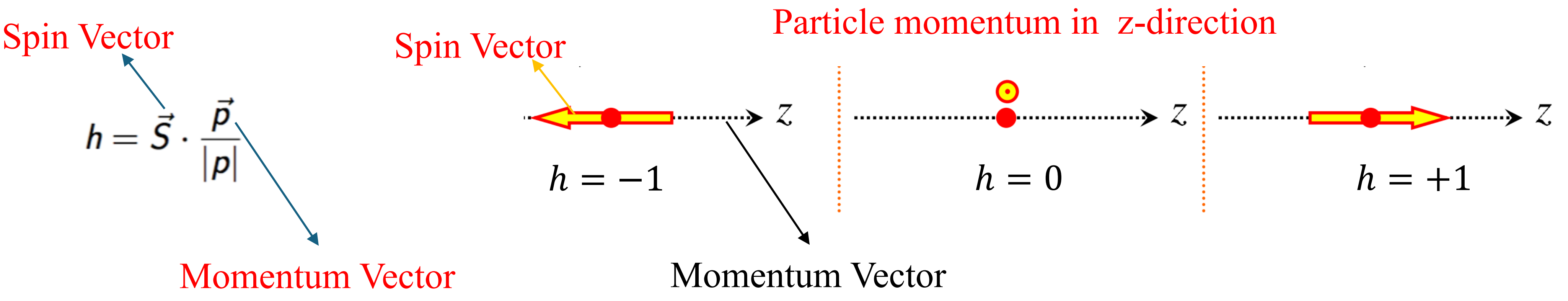

Why do we want to measure diboson polarization?

Massive gauge bosons gain an extra longitudinal degree of freedom via Higgs Mechanism along with the transverse ones.

Polarization: alignment of a particle's spin with its momentum. This is quantified by helicity (h).

- For transverse polarization (T), $h = \pm 1$. Like the two polarizations observed in photon (which is massless)
- **For the longitudinal polarization *(0 or L)*, $h = 0$. Additional degree of freedom present for massive gauge bosons.**

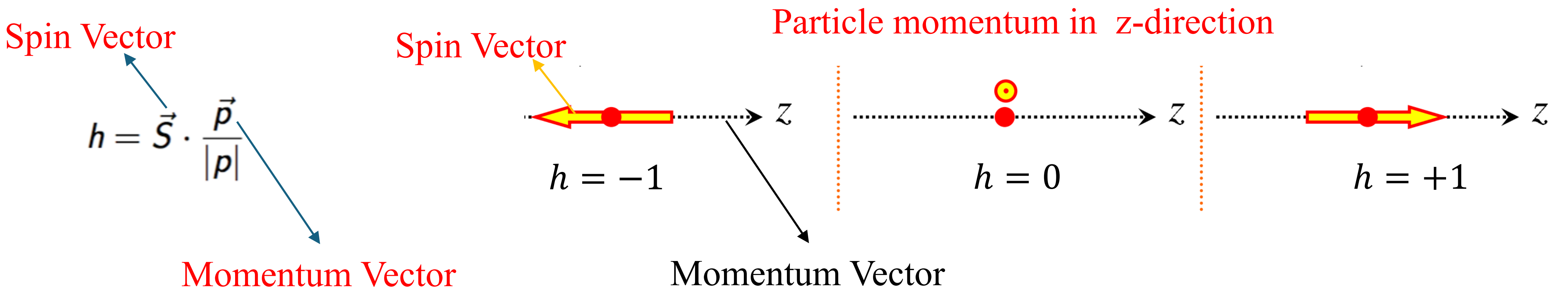

The study of longitudinal vector bosons ($V_0 V_0$ or 00) is an important test of Electroweak Symmetry Breaking.

Why do we want to measure diboson polarization?

New Physics: V_0V_0 (or V_LV_L) production is sensitive to the new physics at high energies [1].

	SM	BSM
$q_{L,R}\bar{q}_{L,R} \to V_L V_L(h)$	~ 1	$\sim E^2/M^2$
$q_{L,R}\bar{q}_{L,R} \to V_\pm V_L(h)$	$\sim m_W/E$	$\sim m_W E/M^2$
$q_{L,R}\bar{q}_{L,R} \to V_\pm V_\pm$	$\sim m_W^2/E^2$	$\sim E^2/M^2$
$q_{L,R}\bar{q}_{L,R} \to V_\pm V_\mp$	~ 1	~ 1

High-energy scaling of diboson in the SM and in BSM (parametrized by d = 6 operators suppressed with new physics at scale M).

Ref [1]: R. Franceschini, G. Panico, A. Pomarol, F. Riva and A. Wulzer, JHEP 02 (2018) 111, Ref [2]: D. Liu and L.-T. Wang, Phys. Rev. D99 (2019) 055001

Why do we want to measure diboson polarization?

New Physics: $V_0 V_0$ production is sensitive to the new physics at high energies [1].

	SM	BSM
$\boxed{q_{L,R}\bar{q}_{L,R} \to V_L V_L(h)}$	$\boxed{\sim 1}$	$\boxed{\sim E^2/M^2}$
$q_{L,R}\bar{q}_{L,R} \to V_\pm V_L(h)$	$\sim m_W/E$	$\sim m_W E/M^2$
$q_{L,R}\bar{q}_{L,R} \to V_\pm V_\pm$	$\sim m_W^2/E^2$	$\sim E^2/M^2$
$q_{L,R}\bar{q}_{L,R} \to V_\pm V_\mp$	~ 1	~ 1

High-energy scaling of diboson in the SM and in BSM (parametrized by d = 6 operators suppressed with new physics at scale *M*).

- f_{00} already measured by ATLAS in inclusive WZ (no cuts applied for enhancing 00 contribution): (PLB 843 (2023) 137895).
  - $f_{00} = 6.7\%$
  - Obs (Exp) significance: 7.1 σ (6.2 σ)
- **Interesting to study the phase spaces where longitudinal-longitudinal (00) contribution is enhanced.**
- **Goal is to reduce the other polarization contributions (0T, T0, TT) and increase that of 00.**

Ref [1]: R. Franceschini, G. Panico, A. Pomarol, F. Riva and A. Wulzer, JHEP 02 (2018) 111, Ref [2]: D. Liu and L.-T. Wang, Phys. Rev. D99 (2019) 055001

Choosing Leptonic WZ

s-channel

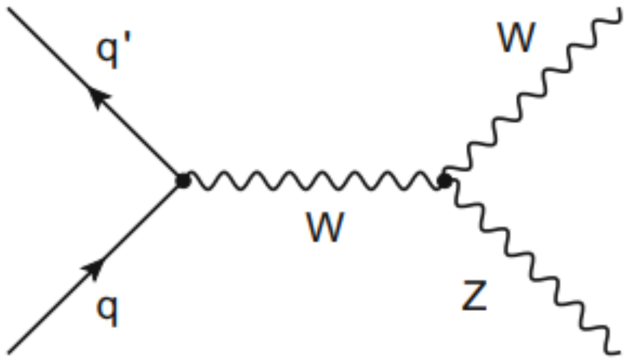

t-channel

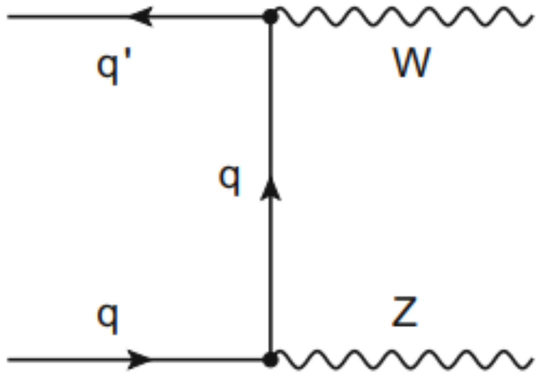

u-channel

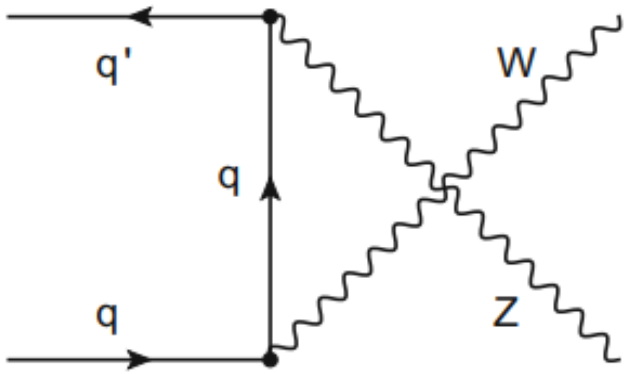

Reasons for choosing WZ production:

1. Comparatively large production cross-section and low instrumental background

2. Most of the kinematics are available with fully-leptonic channels

3. **Helps enhance longitudinal-longitudinal contribution.**
    1. Radiation Amplitude Zero effect
    2. With a high p_T boson selection, further reduces the forward scattering contribution from the transverse-transverse polarization state.

Radiation Amplitude Zero Effect (RAZ)

- Observed in Transverse-Transverse (TT) events of WZ.

Ref [1]: R. Franceschini, G. Panico, A. Pomarol, F. Riva and A. Wulzer, JHEP 02 (2018) 111 Ref [4]: A. Tumasyan *et al.* (CMS Collaboration) Phys. Rev. D 105, 052003 , Ref [5]: V. M. Abazov *et al.* (D0 Collaboration) Phys. Rev. Lett. 100, 241805

Radiation Amplitude Zero Effect (RAZ)

- Observed in Transverse-Transverse (TT) events of WZ.
- As $\cos\theta_W$ approaches 0, σ_{WZ}^{TT} approaches 0 and σ_{WZ}^{0T} and σ_{WZ}^{T0} experience strong gauge cancellations [1]. This effect cannot be seen for events with jets.

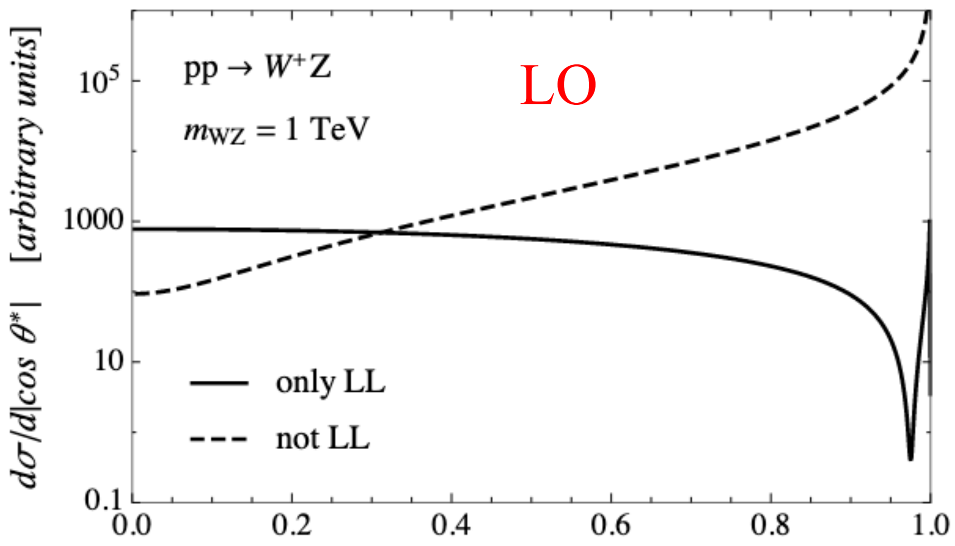

$\cos\theta_W$

Ref [1]: R. Franceschini, G. Panico, A. Pomarol, F. Riva and A. Wulzer, JHEP 02 (2018) 111 Ref [4]: A. Tumasyan *et al.* (CMS Collaboration) Phys. Rev. D 105, 052003 , Ref [5]: V. M. Abazov *et al.* (D0 Collaboration) Phys. Rev. Lett. 100, 241805

Radiation Amplitude Zero Effect (RAZ)

- Observed in Transverse-Transverse (TT) events of WZ.
- As $\cos\theta_W$ approaches 0, σ_{WZ}^{TT} approaches 0 and σ_{WZ}^{0T} and σ_{WZ}^{T0} experience strong gauge cancellations [1]. This effect cannot be seen for events with jets.
- Applying $p_T^{WZ} < X\ GeV$ enhances the RAZ.

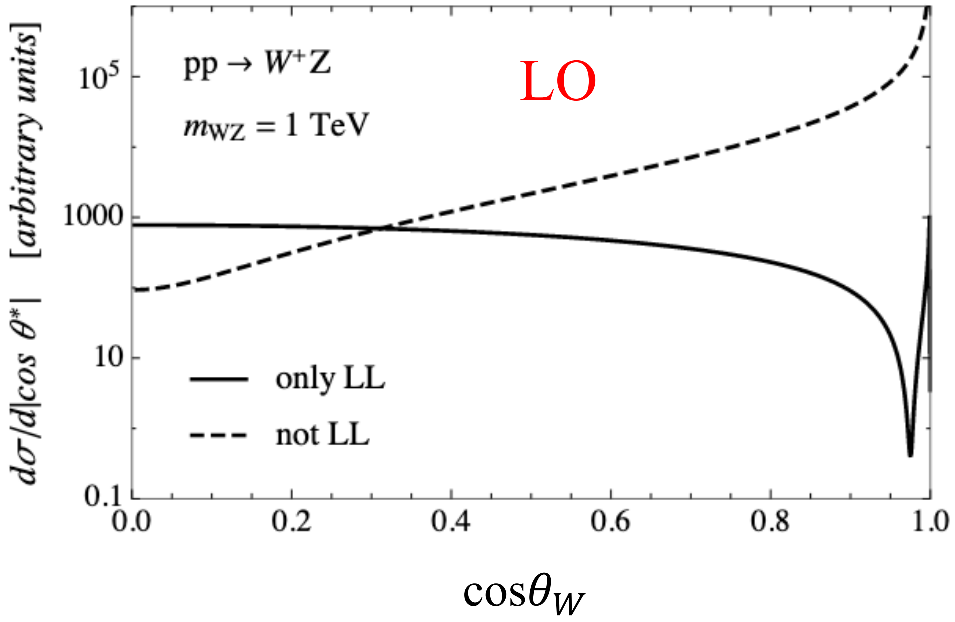

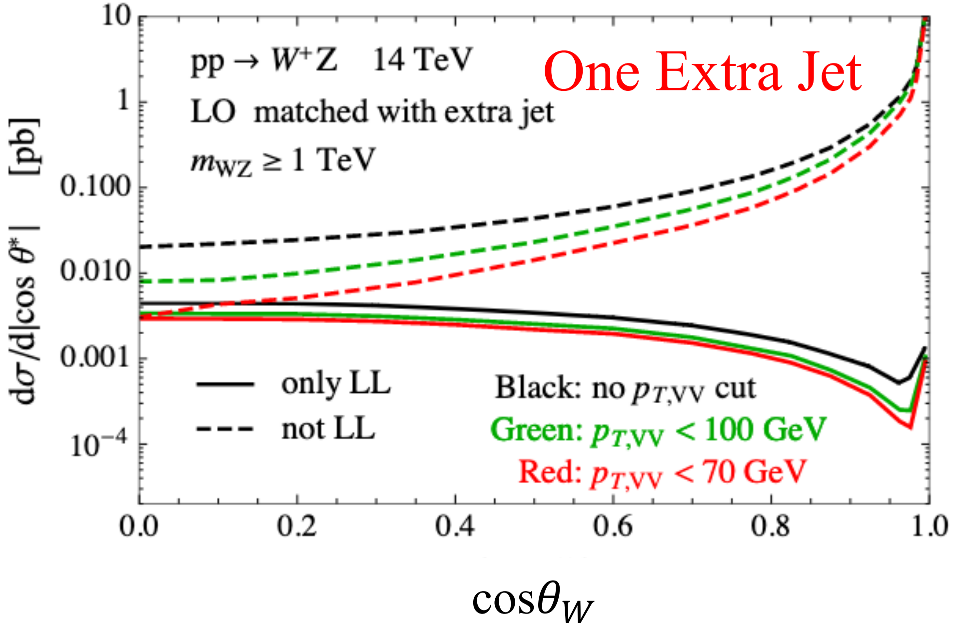

Ref [1]: R. Franceschini, G. Panico, A. Pomarol, F. Riva and A. Wulzer, JHEP 02 (2018) 111 Ref [3]: A. Tumasyan *et al.* (CMS Collaboration) Phys. Rev. D 105, 052003 , Ref [4]: V. M. Abazov *et al.* (D0 Collaboration) Phys. Rev. Lett. 100, 241805

Radiation Amplitude Zero Effect (RAZ)

- Observed in Transverse-Transverse (TT) events of WZ.
- As $\cos\theta_W$ approaches 0, σ_{WZ}^{TT} approaches 0 and σ_{WZ}^{0T} and σ_{WZ}^{T0} experience strong gauge cancellations [1]. This effect cannot be seen for events with jets.
- Applying $p_T^{WZ} < X\ GeV$ enhances the RAZ.

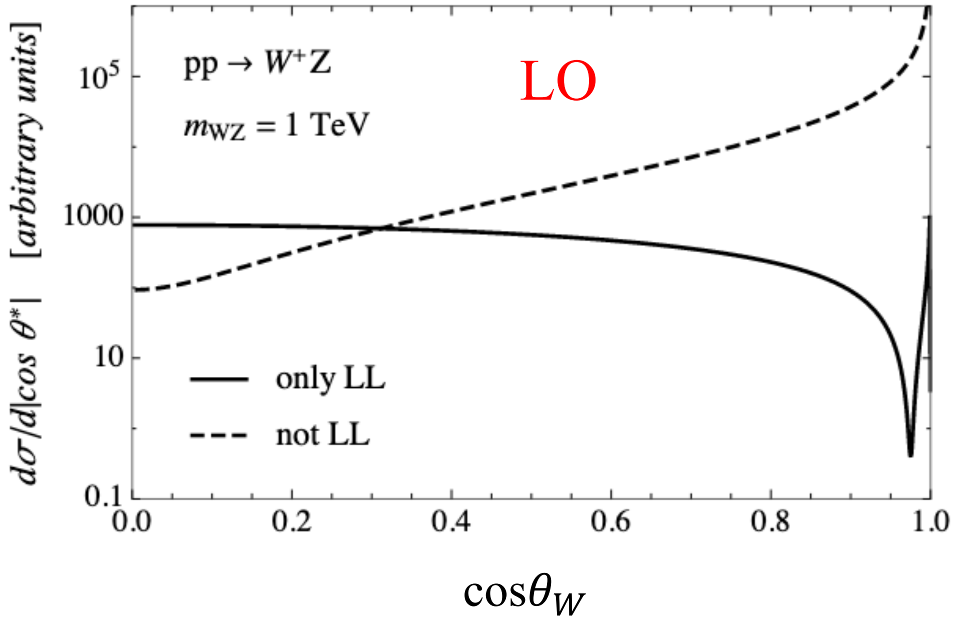

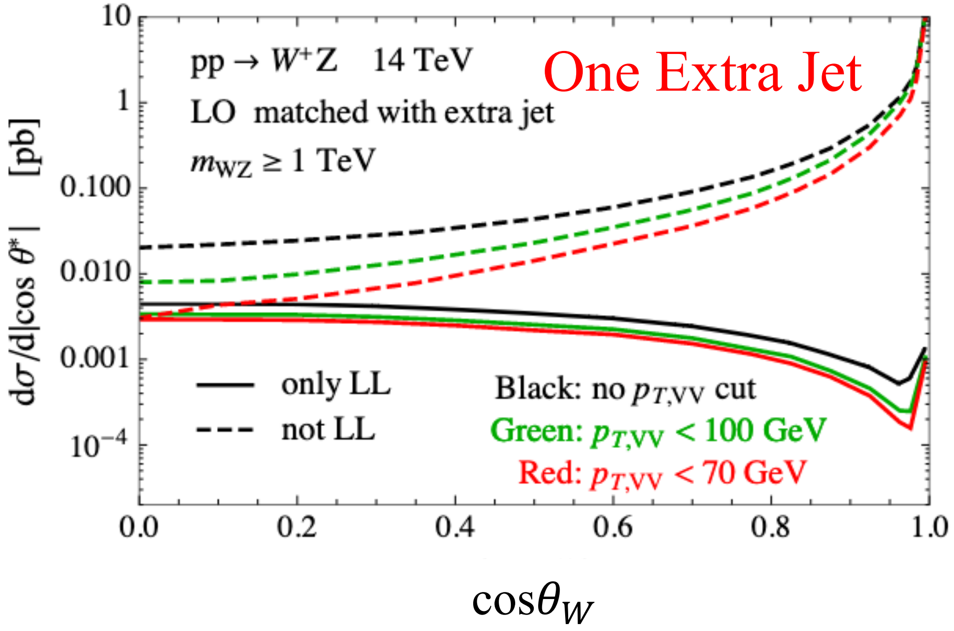

- Only observed for WZ and Wγ but not WW or ZZ.
- Experimentally observed in Wγ[3][4]. This analysis measures RAZ in WZ for the first time
- Need a strategy to reduce jet activity for the measurement.

Ref [1]: R. Franceschini, G. Panico, A. Pomarol, F. Riva and A. Wulzer, JHEP 02 (2018) 111 Ref [3]: A. Tumasyan *et al.* (CMS Collaboration) Phys. Rev. D 105, 052003 , Ref [4]: V. M. Abazov *et al.* (D0 Collaboration) Phys. Rev. Lett. 100, 241805

Signal Regions:

Inclusive region selection

+

Signal regions			
Selection	**Radiation Amplitude Zero**	**00-enhanced region 1**	**00-enriched region 2**
Pass inclusive WZ event selection	✓	✓	✓
Transverse momentum of the Z boson (p_T^Z)	-	$[100, 200]$ GeV	> 200 GeV
Transverse momentum of the WZ system (p_T^{WZ})	$< 20, 40, 70$ GeV	< 70 GeV	

For reducing Jet Activity
to measure RAZ in TT.

Reduces backgrounds including TT
for further enhancing 00.

In the 00-enhanced regions, the 00 fraction is expected to increase by a factor of 2.5 – 4 compared to if these cuts are not applied.

Backgrounds:

Signal regions			
Selection	**Radiation Amplitude Zero**	**00-enhanced region 1**	**00-enriched region 2**
Pass inclusive WZ event selection	✓	✓	✓
Transverse momentum of the Z boson (p_T^Z)	-	$[100, 200]$ GeV	> 200 GeV
Transverse momentum of the WZ system (p_T^{WZ})	$< 20, 40, 70$ GeV	< 70 GeV	

% Compared to the total signal process (00+0T+T0+TT)

Irreducible background (with all prompt leptons) are estimated using the Monte Carlo simulation: $ZZ, VVV, WZ\ EW$ and $t\bar{t}V$	6-11%	12-13%
Reducible background (mainly $t\bar{t}$ and $Z + jets$) with at least one fake lepton is estimated using a data-driven matrix method.	2.5-7%	1-4.5%

Polarized Samples and Higher Order Corrections:

- The MadGraph sample generation is done with LO with two processes (0 jet+1 jet) added together.
- Different polarization states are produced separately.
- The NLO QCD+EW corrections are added using theoretical calculations produced by theorists[6].

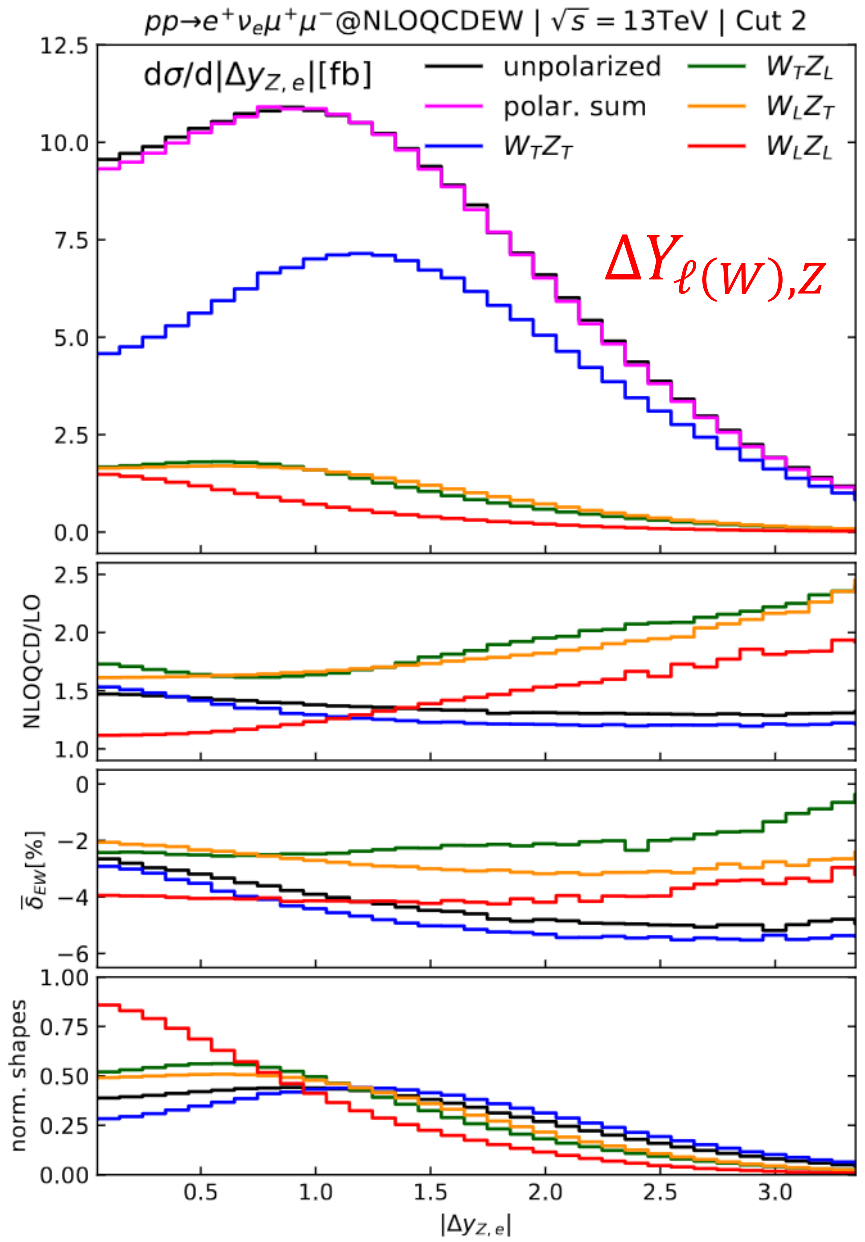

$p_T^{WZ} < 70$ GeV (RAZ)

(NLO QCD)/LO

% δ(EW) wrt NLO QCD

Shapes

Ref [5]: Thi Nhung Dao, Duc Ninh Le **“Enhancing the doubly-longitudinal polarization in WZ production at the LHC”** arXiv:2302.03324 .

How to measure RAZ Experimentally?

- Experimentally $\Delta Y(W,Z)$ and $\Delta Y(\ell_W, Z)$ in TT can be used to measure the RAZ effect

RAZ Signal Region ($p_T^{WZ} < 70$ GeV) i.e. after removing some jet activity

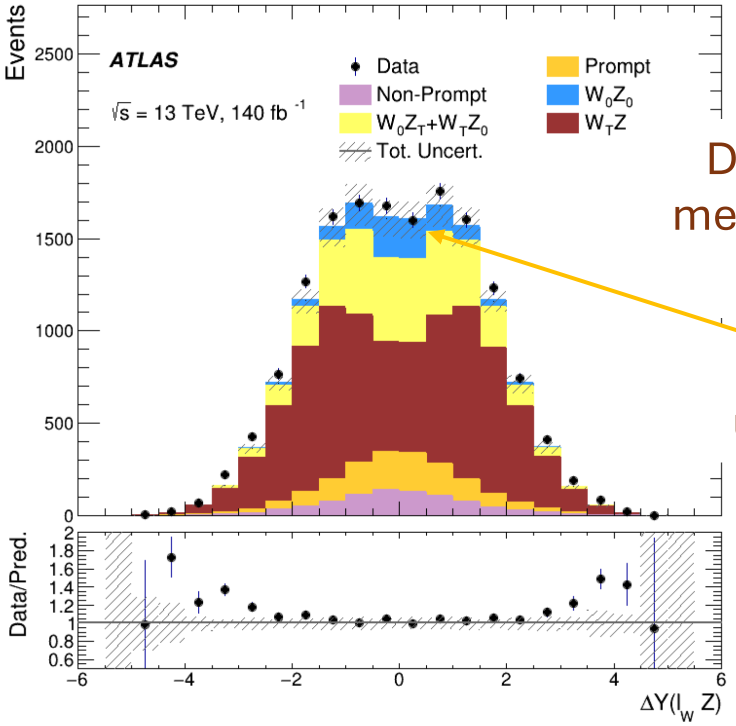

Dip in ΔY can be measured with only $W_T Z_T$ (TT)

Not in unpolarized ΔY

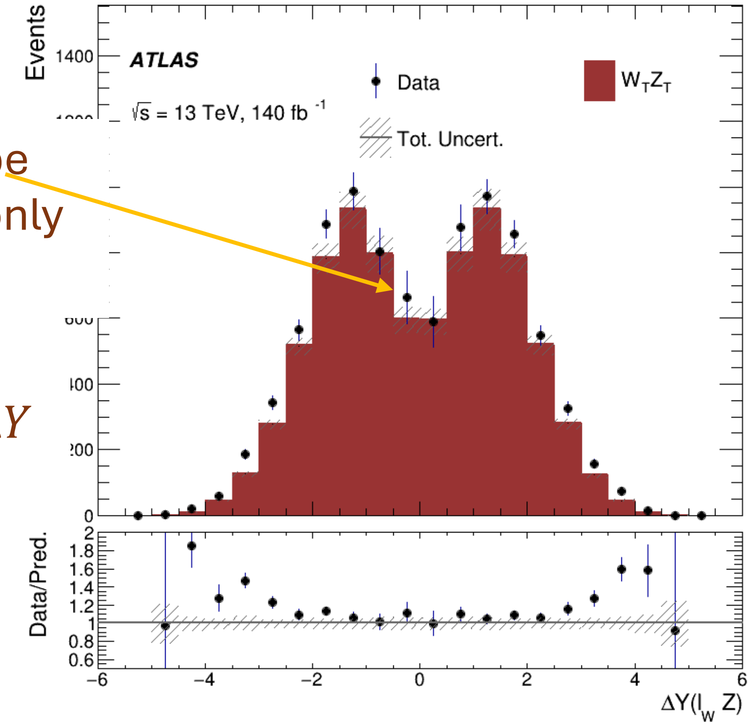

Measurement of Radiation Amplitude Zero

- Depth variable is defined to measure the depth of the dip observed in the rapidity difference distributions for TT events

$$\mathcal{D} = 1 - \frac{N(|\Delta Y|<0.5)}{\left(\frac{N(0.5<|\Delta Y|<1.5)}{2}\right)} = 1 - \frac{2B}{(A+C)}$$

$D > 0$ for a dip, $D < 0$ for a peak

- Measured as a function of the p_T^{WZ} cut (<20, 40, 70 GeV).

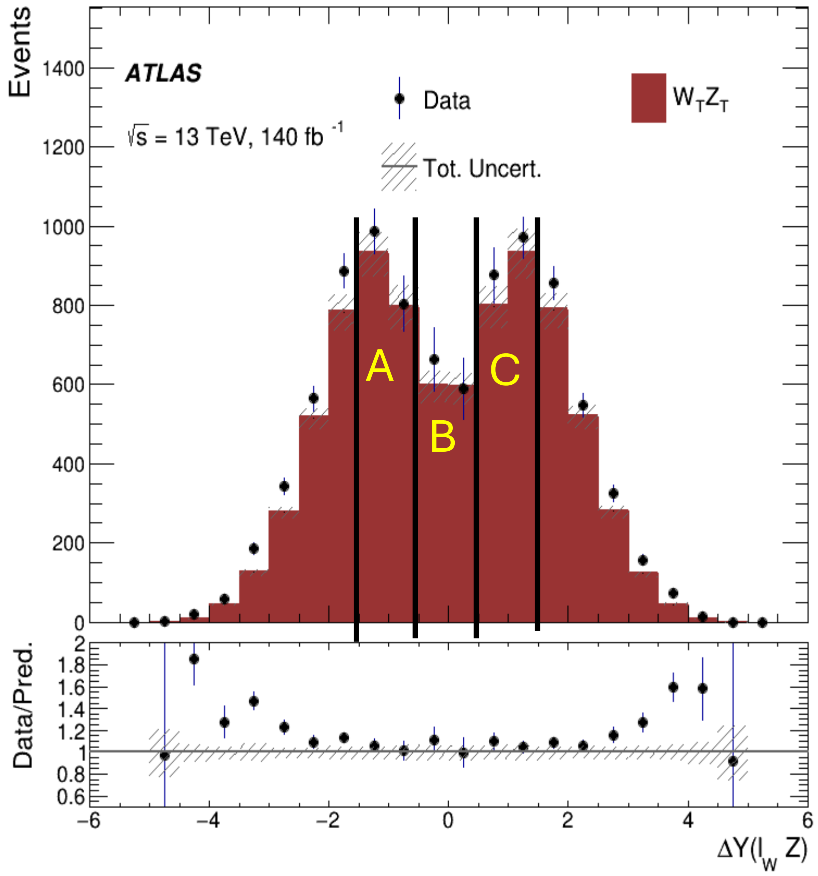

Measurement of Radiation Amplitude Zero

Using Rapidity Difference between lepton of W and Z: $\Delta Y(\ell(W), Z)$

Data-bkg(including 00 0T T0) giving TT contributions compared with the MC.

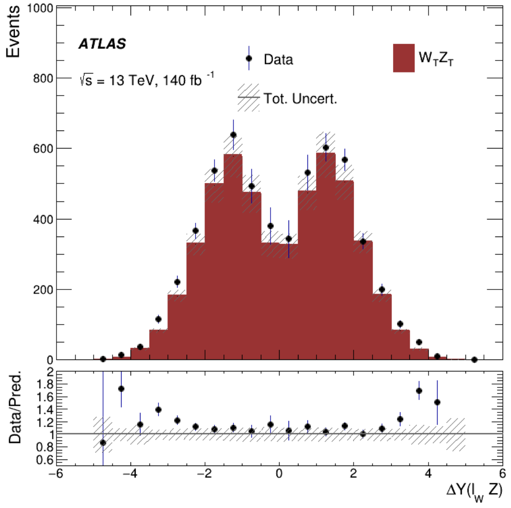

$p_T^{WZ} < 20$ GeV

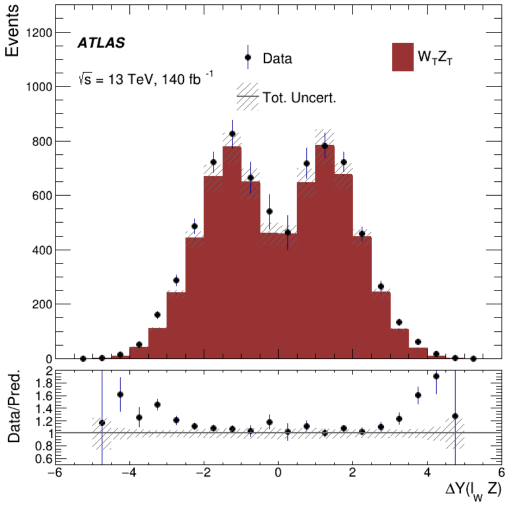

$p_T^{WZ} < 40$ GeV

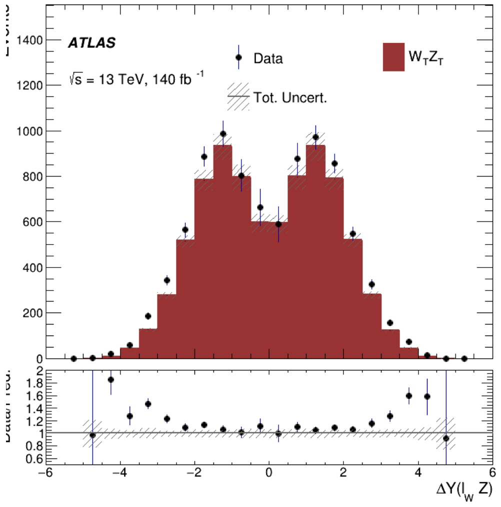

$p_T^{WZ} < 70$ GeV

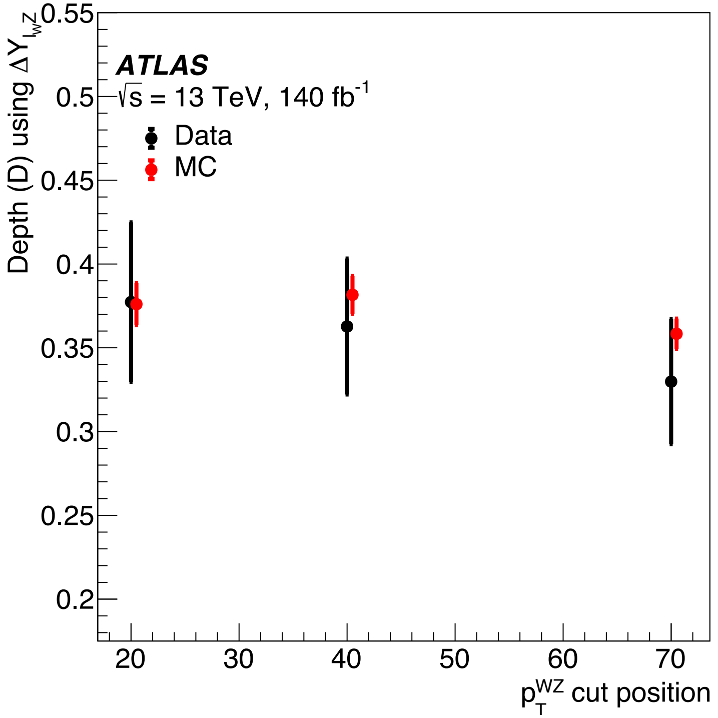

Unfolding

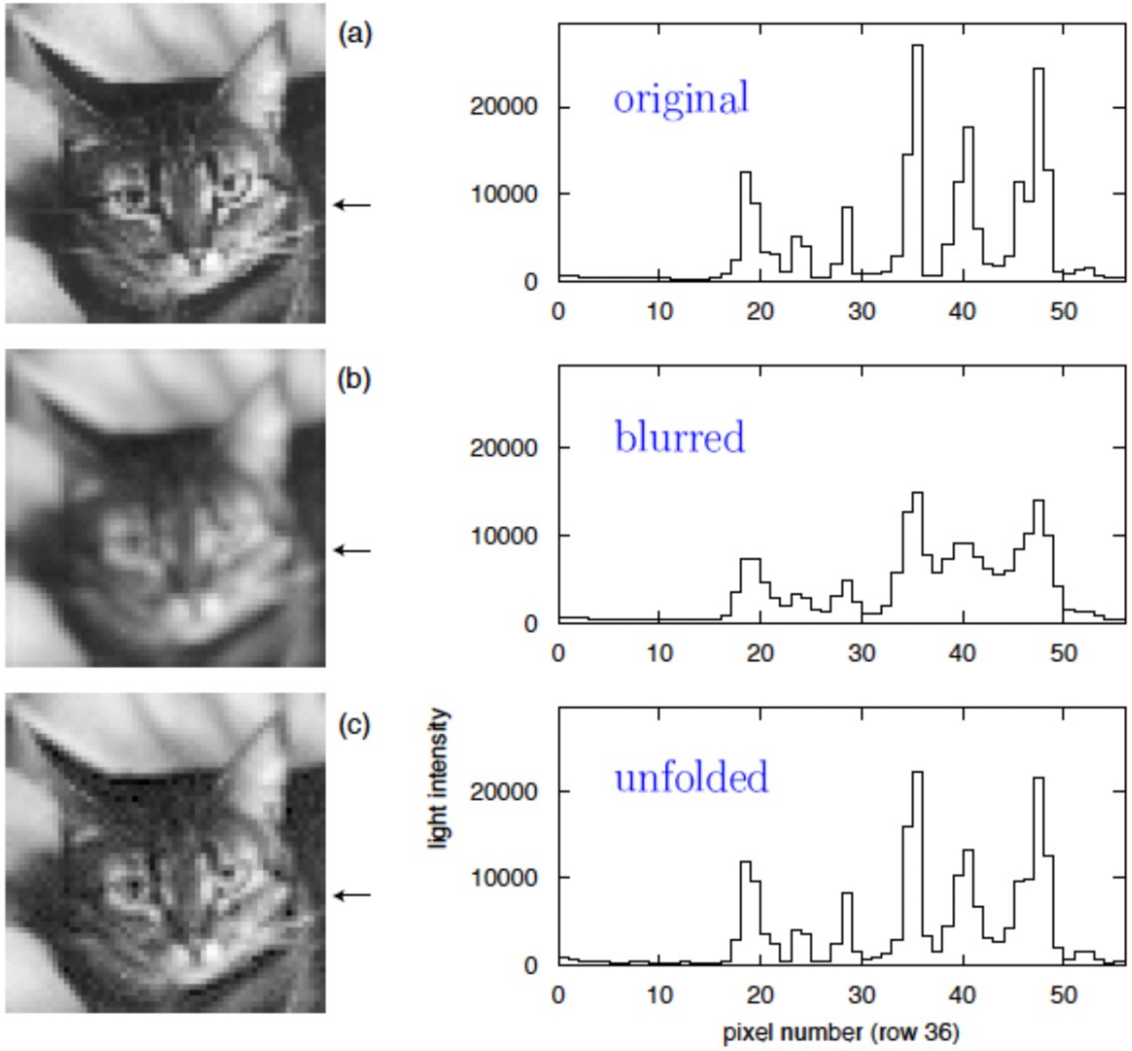

Truth

After going through the detector and reconstruction

Estimating the Truth back

https://agenda.infn.it/event/5719/contributions/60045/attachments/43308/51386/cowan_vietri.pdf

Unfolded Distributions

Unfolding of $\Delta Y(\ell_W, Z)$Distributions

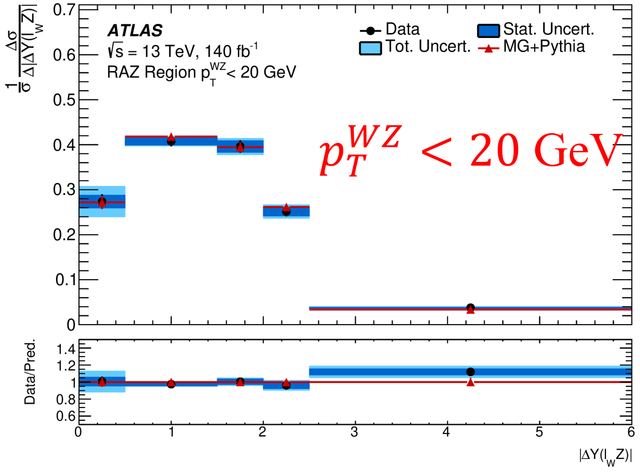

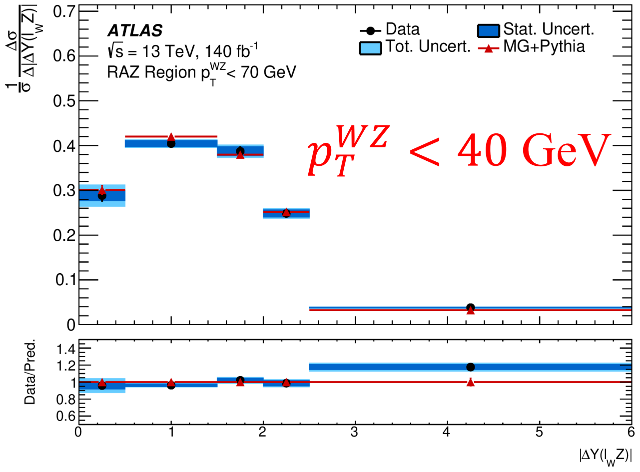

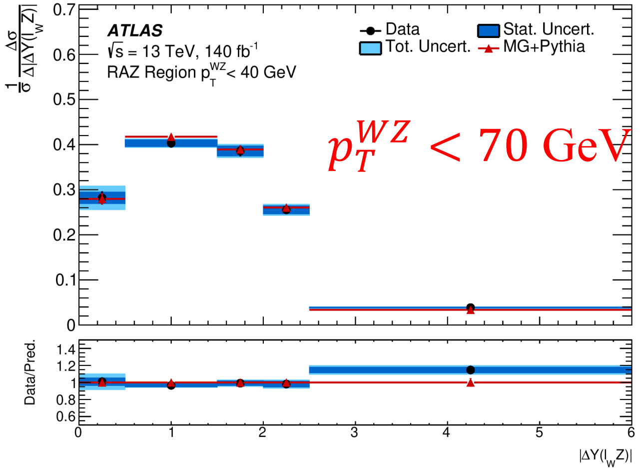

- Unfolding rapidity difference distributions which are compared with the truth.
- Then calculate the depth variable.
- Iterative Bayesian approach is used for unfolding.

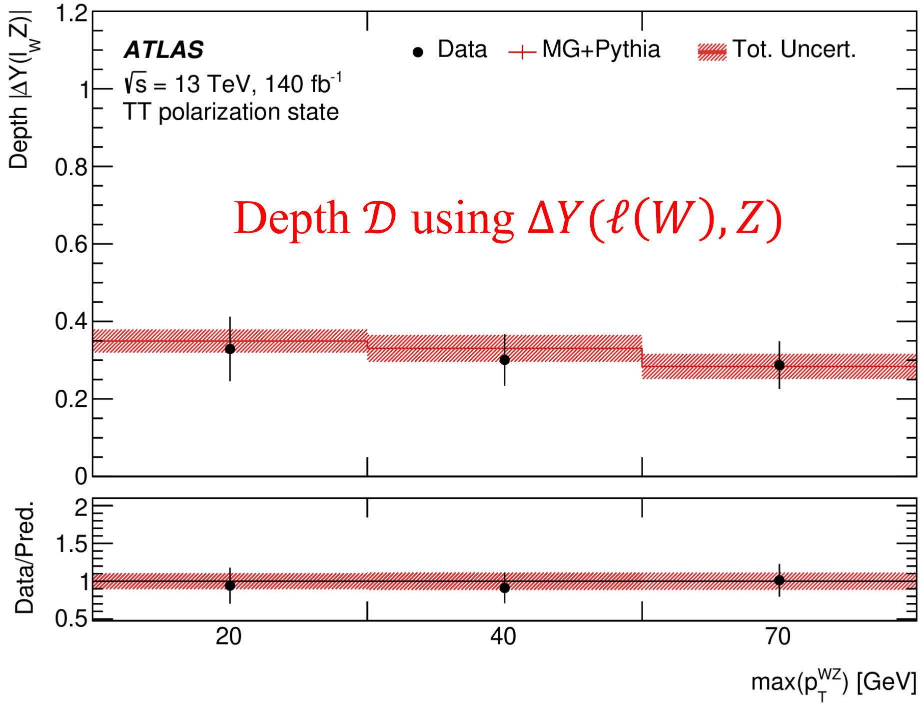

Fraction Measurement in High $p_T(Z)$ Regions

- Use BDTs to increase separation power between 00 and other polarizations
- BDT Training performed separately in the two exclusive high $p_T(Z)$ regions: (100,200] GeV and 200 GeV

$100 < p_T(Z) \leq 200$ GeV

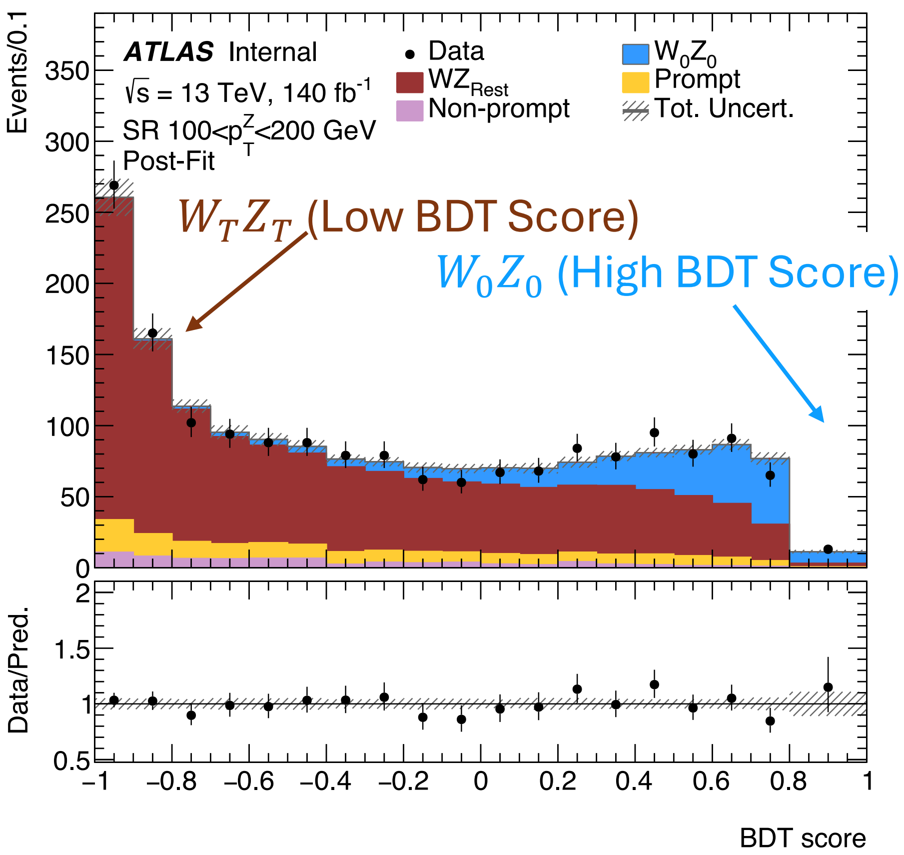

Fraction Measurement in High $p_T(Z)$ Regions

- Use BDTs to increase separation power between 00 and other polarizations
- BDT Training performed separately in the two exclusive high $p_T(Z)$ regions: (100,200] GeV and 200 GeV
- Binned maximum-likelihood fit in separate regions.

Inclusive Phase Space
$f_{00} \approx 7\%$
(PLB 843 (2023) 137895)

High $p_T(Z)$ Phase Space
$f_{00} \approx 16 - 17\%$
arXiv:2402.16365

	Measurement	
	$100 < p_T^Z \leq 200$ GeV	$p_T^Z > 200$ GeV
f_{00}	$0.17 \pm^{0.02}_{0.02}$ (stat) $\pm^{0.01}_{0.02}$ (syst)	$0.16 \pm^{0.05}_{0.05}$ (stat) $\pm^{0.02}_{0.03}$ (syst)
f_{XX}	$0.83 \pm^{0.02}_{0.02}$ (stat) $\pm^{0.02}_{0.01}$ (syst)	$0.84 \pm^{0.05}_{0.05}$ (stat) $\pm^{0.03}_{0.02}$ (syst)
f_{00} obs (exp) sig.	$\boxed{7.7\ (6.9)\ \sigma}$	$\boxed{3.2\ (4.2)\ \sigma}$

$100 < p_T(Z) \leq 200$ GeV

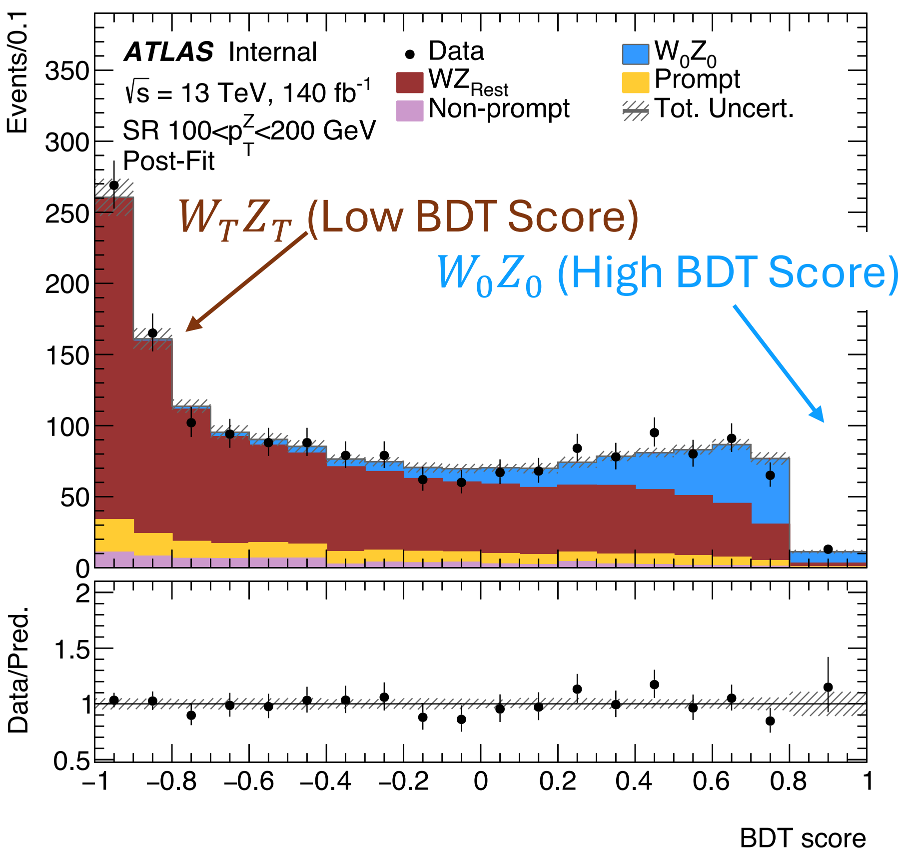

Summary

- The first Radiation Amplitude Zero Effect measurement using WZ events.
  - The two variables sensitive to the RAZ effect ($\Delta Y(\ell_W, Z)$ and $\Delta Y(WZ)$) are unfolded.

- The first measurement of polarization fractions in the two 00-enhanced high $p_T(Z)$ exclusive SRs.

- With these measurements, ATLAS has paved a way to study diboson polarizations and a tool to look for BSM physics in the electroweak sector.

Thank you ☺

Questions?

Motivation: New Physics

Sensitivity to new physics:

	SM	BSM
$q\bar{q} \to V_0 V_0$	~ 1	$\sim E^2/M^2$
$q\bar{q} \to V_\pm V_0$	$\sim m_W/E$	$\sim m_W E/M^2$
$q\bar{q} \to V_\pm V_\pm$	$\sim m_W^2/E^2$	$\sim E^2/M^2$
$q\bar{q} \to V_\pm V_\mp$	~ 1	~ 1

- $V_0 V_0$ production is sensitive to the new physics at high energies [1].

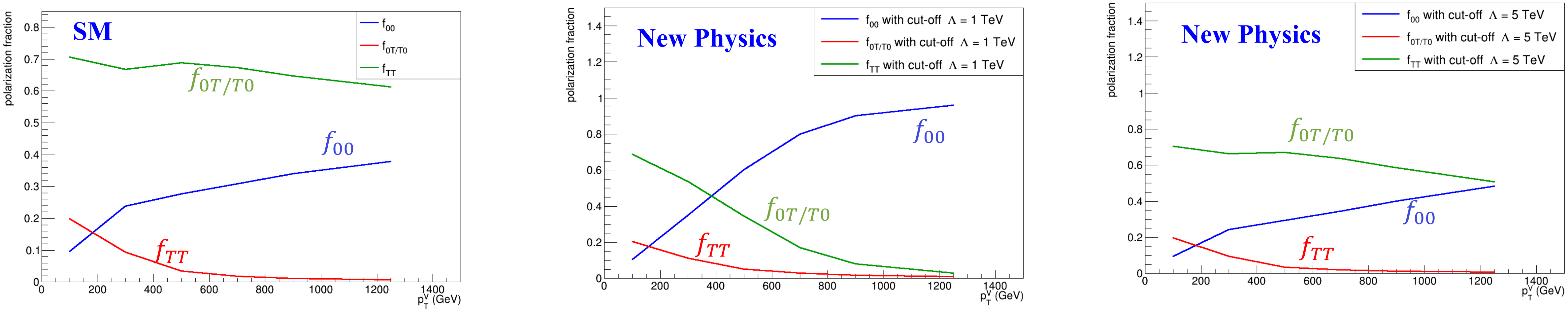

Polarization fractions as a function of p_T^V for SM and a new physics model with a cut off $\Lambda = 1\,TeV$ and $\Lambda = 5\,TeV$ [2]

Ref [1]: R. Franceschini, G. Panico, A. Pomarol, F. Riva and A. Wulzer, JHEP 02 (2018) 111, Ref [2]: D. Liu and L.-T. Wang, Phys. Rev. D99 (2019) 055001

Motivation: EFT Framework

TABLE I. High-energy behavior for the helicity amplitudes $q\bar{q} \to W^+W^-$, where we omit the gauge couplings g^2, g'^2 in front of the amplitudes [32]. $\mathcal{O}_{2W,2B}$ has similar behavior as $\mathcal{O}_{W,B}$. E can be thought as half of the partonic center-of-mass energy (i.e., the energy of a single W boson). For the zeros in the table, the corresponding amplitudes are zero in the zero mass limit. For the WZ final state, the only nonzero amplitudes are those from the left-handed quarks. In addition, only the $\mathcal{O}_{W,HW}$ operators have energy growing behavior in the purely longitudinal helicity state.

(h_{W^+}, h_{W^-})	SM	$\mathcal{O}_W$	$\mathcal{O}_{HW}$	$\mathcal{O}_B$	$\mathcal{O}_{HB}$	$\mathcal{O}_{3W}$
			$q_L\bar{q}_R \to W^+W^-$			
$(\pm,\mp)$	1	0	0	0	0	0
(0,0)	1	$\frac{E^2}{\Lambda^2}$	$\frac{E^2}{\Lambda^2}$	$\frac{E^2}{\Lambda^2}$	$\frac{E^2}{\Lambda^2}$	0
$(0,\pm),(\pm,0)$	$\frac{m_W}{E}$	$\frac{Em_W}{\Lambda^2}$	$\frac{Em_W}{\Lambda^2}$	$\frac{Em_W}{\Lambda^2}$	$\frac{Em_W}{\Lambda^2}$	$\frac{Em_W}{\Lambda^2}$
$(\pm,\pm)$	$\frac{m_W^2}{E^2}$	$\frac{m_W^2}{\Lambda^2}$	$\frac{m_W^2}{\Lambda^2}$	$\frac{m_W^2}{\Lambda^2}$	0	$\frac{E^2}{\Lambda^2}$
			$q_R\bar{q}_L \to W^+W^-$			
$(\pm,\mp)$	0	0	0	0	0	0
(0,0)	1	$\frac{m_W^2}{\Lambda^2}$	$\frac{m_W^2}{\Lambda^2}$	$\frac{E^2}{\Lambda^2}$	$\frac{E^2}{\Lambda^2}$	0
$(0,\pm),(\pm,0)$	$\frac{m_W}{E}$	$\frac{m_W^2 m_Z^2}{\Lambda^2 E^2}$	$\frac{Em_W}{\Lambda^2}$	$\frac{Em_W}{\Lambda^2}$	$\frac{Em_W}{\Lambda^2}$	$\frac{m_W^2 m_Z^2}{\Lambda^2 E^2}$
$(\pm,\pm)$	$\frac{m_W^2}{E^2}$	$\frac{m_W^2}{\Lambda^2}$	$\frac{m_W^2}{\Lambda^2}$	$\frac{m_W^2}{\Lambda^2}$	0	$\frac{m_W^2}{\Lambda^2}$

TABLE II. Observables for probing the higher-dimensional operators. c_f denotes the Wilson coefficients of the fermionic operators in Eq. (2). For reference, we have also included contributions from potential dimension-8 operators with Wilson coefficients denoted by c_{TX}. See Appendix C of Ref. [37] for the definition of the dimension-8 operators.

Observable	$\delta O/O_{\mathrm{SM}}$
$W_L^+W_L^-$	$[(c_W+c_{HW}-c_{2W})T_f^3+(c_B+c_{HB}-c_{2B})Y_f t_w^2]\frac{E^2}{\Lambda^2},\ c_f\frac{E^2}{\Lambda^2}$
$W_T^+W_T^-$	$c_{3W}\frac{m_W^2}{\Lambda^2}+c_{3W}^2\frac{E^4}{\Lambda^4},\ c_{TWW}\frac{E^4}{\Lambda^4}$
$W_L^\pm Z_L$	$(c_W+c_{HW}-c_{2W}+4c_L^{(3)q})\frac{E^2}{\Lambda^2}$
$W_T^\pm Z_T(\gamma)$	$c_{3W}\frac{m_W^2}{\Lambda^2}+c_{3W}^2\frac{E^4}{\Lambda^4},\ c_{TWB}\frac{E^4}{\Lambda^4}$
$W_L^\pm h$	$(c_W+c_{HW}-c_{2W}+4c_L^{(3)q})\frac{E^2}{\Lambda^2}$
Zh	$[(c_W+c_{HW}-c_{2W})T_f^3-(c_B+c_{HB}-c_{2B})Y_f t_w^2]\frac{E^2}{\Lambda^2},\ c_f\frac{E^2}{\Lambda^2}$
Z_TZ_T	$(c_{TWW}+t_w^4 c_{TBB}-2T_f^3 t_w^2 c_{TWB})\frac{E^4}{\Lambda^4}$
$\gamma\gamma$	$(c_{TWW}+c_{TBB}+2T_f^3 c_{TWB})\frac{E^4}{\Lambda^4}$
$\hat{S}$	$(c_W+c_B)\frac{m_W^2}{\Lambda^2}$
$h\to Z\gamma$	$(c_{HW}-c_{HB})\frac{(4\pi v)^2}{\Lambda^2}$
$h\to W^+W^-$	$(c_W+c_{HW})\frac{m_W^2}{\Lambda^2}$

$$c_{q_L}^{(3)} = c_W + c_{HW} - c_{2W} + 4c_L^{(3)q},$$
$$c_{u_L}^{(1)} = c_B + c_{HB} - c_{2B} + 4c_L^q,$$
$$c_{d_L}^{(1)} = c_B + c_{HB} - c_{2B} - 4c_L^q,$$
$$c_{u_R}^{(1)} = c_B + c_{HB} - c_{2B} + 3c_{u_R},$$
$$c_{d_R}^{(1)} = c_B + c_{HB} - c_{2B} - 6c_{d_R}.$$

Ref [2]: D. Liu and L.-T. Wang, Phys. Rev. D99 (2019) 055001

Motivation: New Physics

TABLE VI. Helicity cross sections (in fb) for the diboson processes at the 14 TeV LHC as a function of the cutoff Λ (in TeV) in each p_T bin with the Wilson coefficient c_{HW} set to 1.

σ (fb), p_T (GeV)	[0,200]	[200, 400]	[400,600]
$W_L^\pm Z_L$	$784\ (1+\frac{0.116}{\Lambda^2}+\frac{0.00625}{\Lambda^4})$	$58.5\ (1+\frac{0.682}{\Lambda^2}+\frac{0.141}{\Lambda^4})$	$4.84\ (1+\frac{2.09}{\Lambda^2}+\frac{1.24}{\Lambda^4})$
$W_{L(T)}^\pm Z_{T(L)}$	$1614\ (1+\frac{0.0610}{\Lambda^2}+\frac{0.00181}{\Lambda^4})$	$23.0\ (1+\frac{0.419}{\Lambda^2}+\frac{0.0611}{\Lambda^4})$	$0.598\ (1+\frac{1.40}{\Lambda^2}+\frac{0.623}{\Lambda^4})$
$W_T^\pm Z_T$	5755	164	12.0
$W_L^+ W_L^-$	$1416\ (1+\frac{0.0318}{\Lambda^2}+\frac{0.00203}{\Lambda^4})$	$34.0\ (1+\frac{0.597}{\Lambda^2}+\frac{0.121}{\Lambda^4})$	$2.75\ (1+\frac{1.83}{\Lambda^2}+\frac{1.05}{\Lambda^4})$
$W_{L(T)}^+ W_{T(L)}^-$	$4866\ (1+\frac{0.00758}{\Lambda^2}+\frac{0.000489}{\Lambda^4})$	$34.6\ (1+\frac{0.130}{\Lambda^2}+\frac{0.0207}{\Lambda^4})$	$0.848\ (1+\frac{0.429}{\Lambda^2}+\frac{0.213}{\Lambda^4})$
$W_T^+ W_T^-$	17987	523	39.1
$W_L^\pm h$	$387\ (1+\frac{0.149}{\Lambda^2}+\frac{0.00776}{\Lambda^4})$	$46.5\ (1+\frac{0.712}{\Lambda^2}+\frac{0.148}{\Lambda^4})$	$4.30\ (1+\frac{2.13}{\Lambda^2}+\frac{1.24}{\Lambda^4})$
$W_T^\pm h$	$270\ (1+\frac{0.0302}{\Lambda^2}+\frac{0.000146}{\Lambda^4})$	$4.93\ (1+\frac{0.0287}{\Lambda^2}+\frac{0.000217}{\Lambda^4})$	$0.140\ (1+\frac{0.0271}{\Lambda^2}+\frac{0.000275}{\Lambda^4})$
$Z_L h$	$198\ (1+\frac{0.134}{\Lambda^2}+\frac{0.00731}{\Lambda^4})$	$24.5\ (1+\frac{0.628}{\Lambda^2}+\frac{0.136}{\Lambda^4})$	$2.24\ (1+\frac{1.90}{\Lambda^2}+\frac{1.14}{\Lambda^4})$
$Z_T h$	$154\ (1+\frac{0.0361}{\Lambda^2}+\frac{0.000353}{\Lambda^4})$	$3.30\ (1+\frac{0.0688}{\Lambda^2}+\frac{0.00501}{\Lambda^4})$	$0.0941\ (1+\frac{0.165}{\Lambda^2}+\frac{0.0413}{\Lambda^4})$
σ [fb], p_T [GeV]	[600,800]	[800,1000]	[1000,1500]
$W_L^\pm Z_L$	$0.799\ (1+\frac{4.30}{\Lambda^2}+\frac{4.87}{\Lambda^4})$	$0.188\ (1+\frac{6.92}{\Lambda^2}+\frac{13.4}{\Lambda^4})$	$0.0749\ (1+\frac{11.9}{\Lambda^2}+\frac{39.1}{\Lambda^4})$
$W_{L(T)}^\pm Z_{T(L)}$	$0.0471\ (1+\frac{2.91}{\Lambda^2}+\frac{2.60}{\Lambda^4})$	$0.00634\ (1+\frac{4.89}{\Lambda^2}+\frac{7.34}{\Lambda^4})$	$0.00149\ (1+\frac{8.01}{\Lambda^2}+\frac{20.6}{\Lambda^4})$
$W_T^\pm Z_T$	1.74	0.357	0.121
$W_L^+ W_L^-$	$0.442\ (1+\frac{3.74}{\Lambda^2}+\frac{4.13}{\Lambda^4})$	$0.102\ (1+\frac{6.13}{\Lambda^2}+\frac{11.4}{\Lambda^4})$	$0.0405\ (1+\frac{10.4}{\Lambda^2}+\frac{32.6}{\Lambda^4})$
$W_{L(T)}^+ W_{T(L)}^-$	$0.0652\ (1+\frac{0.888}{\Lambda^2}+\frac{0.889}{\Lambda^4})$	$0.00873\ (1+\frac{1.49}{\Lambda^2}+\frac{2.47}{\Lambda^4})$	$0.00204\ (1+\frac{2.43}{\Lambda^2}+\frac{6.79}{\Lambda^4})$
$W_T^+ W_T^-$	5.92	1.28	0.475
$W_L^\pm h$	$0.726\ (1+\frac{4.22}{\Lambda^2}+\frac{4.83}{\Lambda^4})$	$0.169\ (1+\frac{7.15}{\Lambda^2}+\frac{13.3}{\Lambda^4})$	$0.0671\ (1+\frac{12.2}{\Lambda^2}+\frac{38.7}{\Lambda^4})$
$W_T^\pm h$	$0.0112\ (1+\frac{0.0283}{\Lambda^2}+\frac{0.000218}{\Lambda^4})$	0.00153	0.000364
$Z_L h$	$0.367\ (1+\frac{3.82}{\Lambda^2}+\frac{4.50}{\Lambda^4})$	$0.0835\ (1+\frac{6.27}{\Lambda^2}+\frac{12.4}{\Lambda^4})$	$0.0327(1+\frac{11.0}{\Lambda^2}+\frac{35.9}{\Lambda^4})$
$Z_T h$	$0.00737\ (1+\frac{0.318}{\Lambda^2}+\frac{0.165}{\Lambda^4})$	$0.000991\ (1+\frac{0.523}{\Lambda^2}+\frac{0.455}{\Lambda^4})$	$0.000231\ (1+\frac{0.838}{\Lambda^2}+\frac{1.24}{\Lambda^4})$

Ref [2]: D. Liu and L.-T. Wang, Phys. Rev. D99 (2019) 055001

Radiation Amplitude Zero: Amplitudes

$$f_1(p_1)\,\bar{f}_2(p_2) \to W(p_W)\,Z(p_Z)\,,$$

$$\mathcal{M}(\lambda_W,\lambda_Z) = \frac{F}{s}\,\overline{V}(p_2)\left[X\left(\not{A} - \frac{t}{s-M_W^2}\not{V}\right) + Y\not{V}\right] \times (1-\gamma_5)\,U(p_1)\,, \qquad (4)$$

where X and Y are combinations of coupling factors

$$X = \frac{s}{2}\left(\frac{g_-^{f_1}}{u} + \frac{g_-^{f_2}}{t}\right), \quad Y = g_-^{f_1}\,\frac{M_Z^2\, s}{2\,u\,(s-M_W^2)}\,,$$

where λ_W (λ_Z) denotes the W (Z) boson polarization ($\lambda = \pm 1, 0$ for transverse and longitudinal polarizations, respectively)

$$\mathcal{M}(\pm,\mp) = F\sin\theta(\lambda_W - \cos\theta)X,$$

$$\mathcal{M}(\pm,\pm) = F\sin\theta\left[\left(\lambda_W(r_Z - r_W) - \beta + \cos\theta + \beta\frac{\alpha-\beta\cos\theta}{1-r_W}\right)X + 2\beta Y\right],$$

$$\mathcal{M}(0,0) = F\frac{\sin\theta}{\sqrt{2r_W 2r_Z}}\left[\left(-\beta\rho + \beta_W\beta_Z\cos\theta + \beta\rho\frac{\alpha-\beta\cos\theta}{1-r_W}\right)X + 2\beta\rho Y\right],$$

$$\mathcal{M}(\pm,0) = F\frac{1-\lambda_W\cos\theta}{\sqrt{2r_Z}}\left[\left(2\lambda_W r_Z - \beta + \beta_Z\cos\theta + \beta\frac{\alpha-\beta\cos\theta}{1-r_W}\right)X + 2\beta Y\right],$$

$$\mathcal{M}(0,\pm) = F\frac{1+\lambda_Z\cos\theta}{\sqrt{2r_W}}\left[\left(-2\lambda_Z r_W - \beta + \beta_W\cos\theta + \beta\frac{\alpha-\beta\cos\theta}{1-r_W}\right)X + 2\beta Y\right].$$

The amplitudes given in Eqs. (5)–(9) exhibit several interesting features. $\mathcal{M}(\pm,\mp)$ receive contributions only from $J \geq 2$ partial waves, i.e., only from the u and t channel fermion-exchange diagrams. The $(\pm,\mp)$ amplitudes therefore do not depend on Y and thus factorize. They vanish for

$$\frac{g_-^{f_1}}{u} + \frac{g_-^{f_2}}{t} = 0 \quad\text{or}\quad \cos\theta_0 = \frac{\alpha}{\beta}\left(\frac{g_-^{f_1}+g_-^{f_2}}{g_-^{f_1}-g_-^{f_2}}\right).$$

The existence of the zero in $\mathcal{M}(\pm,\mp)$ at $\cos\theta_0$ is a direct consequence of the contributing Feynman diagrams and the left-handed coupling of the W boson to fermions. Unlike the $W^\pm\gamma$ case with its massless photon kinematics, the zero has an energy dependence through α and β which is, however, rather weak for energies sufficiently above the WZ mass threshold. More explicitly, for $s \gg M_V^2$, the zero is located at

$$\cos\theta_0 \simeq \begin{cases} \frac{1}{3}\tan^2\theta_W \simeq 0.1 & \text{for } d\bar{u} \to W^-Z\,, \\ -\tan^2\theta_W \simeq -0.3 & \text{for } e^-\bar{\nu}_e \to W^-Z\,. \end{cases}$$

Amplitudes that remain non-zero at high energies i.e. $s \gg M_V^2$ are:

$$\mathcal{M}(\pm,\mp) \longrightarrow \frac{F}{\sin\theta}(\lambda_W - \cos\theta)\left[(g_-^{f_1} - g_-^{f_2})\cos\theta - (g_-^{f_1} + g_-^{f_2})\right],$$

$$\mathcal{M}(0,0) \longrightarrow \frac{F}{2}\sin\theta\,\frac{M_Z}{M_W}(g_-^{f_2} - g_-^{f_1})\,.$$

Ref: U. Baur, T. Han and J. Ohnemus, Amplitude zeros in $W^\pm Z$ production, Phys. Rev. Lett. 72 (1994) 3941

Radiation Amplitude Zero Effect

- At high energies, with $s \gg m_V^2$, the only amplitudes that remain non-zero are (here θ is the θ_W defined in the parton center of mass frame):

$$\mathcal{M}(\pm,\mp) \longrightarrow \frac{F}{\sin\theta}(\lambda_W - \cos\theta)\left[\left(g_-^{f_1} - g_-^{f_2}\right)\cos\theta - \left(g_-^{f_1} + g_-^{f_2}\right)\right],$$
$$\mathcal{M}(0,0) \longrightarrow \frac{F}{2}\sin\theta\frac{m_Z}{m_W}\left(g_-^{f_2} - g_-^{f_1}\right).$$

- The other terms reduce a lot because of strong gauge cancellations. Because of this, an approximate zero is observed at:

$$\cos\theta_0 = \frac{\alpha}{\beta}\left(\frac{g_-^{f_1} + g_-^{f_2}}{g_-^{f_1} - g_-^{f_2}}\right).$$

Which is $cos\theta_0 \simeq {}^1/_3\, tan^2\theta_W \simeq 0.1$ for $d\bar{u} \rightarrow W^-Z$

Here θ_W is the weak mixing angle. And $g_-^{f_1}$ and $g_-^{f_2}$ are the couplings of Z to left-handed fermions. λ_W are the polarization states $(\pm 1, 0)$. (other terms explained in backup)

Ref [6]: U. Baur, Tao Han, and J. Ohnemus. “Amplitude zeros in W+- Z production”. Phys. Rev. Lett. 72 (1994), pp. 3941–3944.

The factor F contains coupling factors, $F = Ce^2/\sqrt{2}\sin\theta_W$, where θ_W is the weak mixing angle, and the color factor $C = \delta_{i_1 i_2} V_{f_1 f_2}$. Here i_1 (i_2) is the color index of the incoming quark (antiquark) and $V_{f_1 f_2}$ is the quark mixing matrix element. The angle θ is the center of mass scattering angle of the W boson with respect to the fermion (f_1) direction. We have $\alpha = 1 - r_W - r_Z$, $\beta = \left(\alpha^2 - 4 r_W r_Z\right)^{1/2}$, $\beta_W = 1 + r_W - r_Z$, $\beta_Z = 1 - r_W + r_Z$, $\rho = 1 + r_W + r_Z$, and $r_V = m_V^2/s$ with $V = W, Z$.

The kinematic variables are defined by:

$$s = (p_1 + p_2)^2, \quad t = (p_1 - p_W)^2 = -\frac{s}{2}(\alpha - \beta\cos\theta), \quad u = (p_1 - p_Z)^2 = -\frac{s}{2}(\alpha + \beta\cos\theta).$$

X and Y are combinations of coupling factors:

$$X = \frac{s}{2}\left(\frac{g_-^{f_1}}{u} + \frac{g_-^{f_2}}{t}\right), \quad Y = g_-^{f_1}\frac{m_Z^2\, s}{2u\left(s - m_W^2\right)},$$

where m_W (m_Z) is the W (Z) boson mass and $g_-^f = \left(T_3^f - \; Q_f \sin^2\theta_W\right)/(\sin\theta_W \cos\theta_W)$ is the coupling of the Z boson to left-handed fermions. Here $T_3^f = \pm\frac{1}{2}$ represents the third component of the weak isospin and Q_f is the electric charge of the fermion f.

Radiation Amplitude Zero: Amplitudes

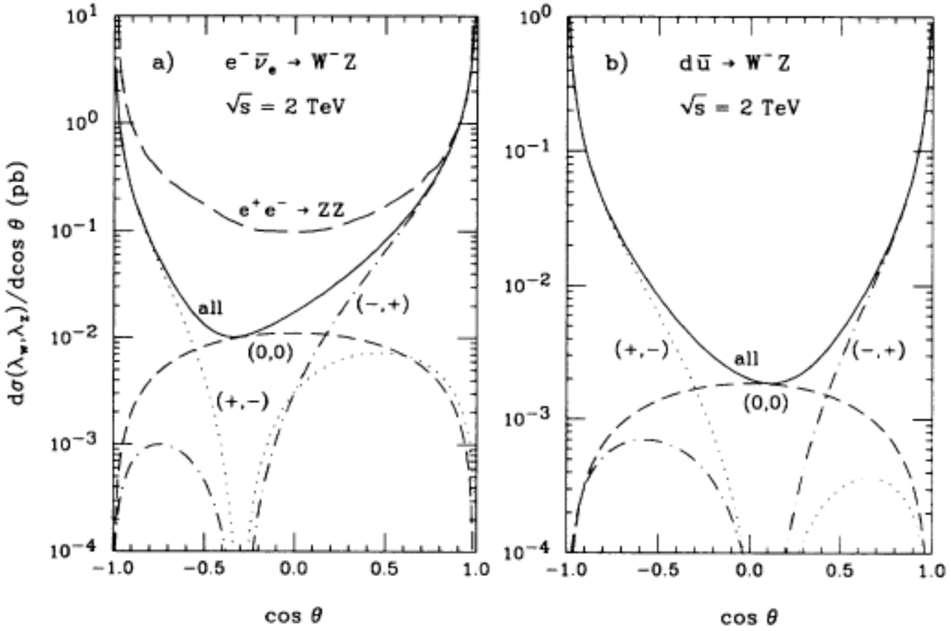

FIG. 1. Differential cross section $d\sigma(\lambda_W, \lambda_Z)/d\cos\theta$ versus the W^- scattering angle θ in the center of mass frame for the Born-level processes (a) $e^- \bar{\nu}_e \to W^- Z$ and (b) $d\bar{u} \to W^- Z$. The dashed, dotted, and dash-dotted curves are for $(\lambda_W, \lambda_Z) = (0,0)$, $(+,-)$, and $(-,+)$, respectively. The solid line represents the total (unpolarized) cross section. For comparison, the long dashed curve in (a) shows the $e^+ e^- \to ZZ$ cross section, normalized to the $e^- \bar{\nu}_e \to W^- Z$ cross section at $\cos\theta = 0.9$.

Ref [5]: U. Baur, T. Han and J. Ohnemus, Amplitude zeros in $W^{\pm}Z$ production, Phys. Rev. Lett. 72 (1994) 3941

Introduction

New Physics: V_0V_0 production is sensitive to the new physics at high energies [1].

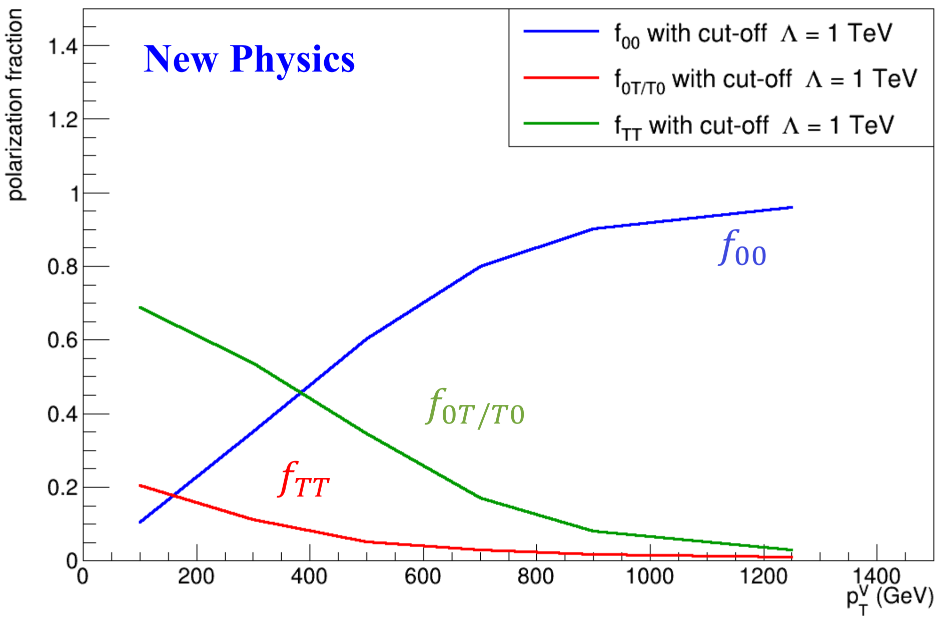

Polarization fractions as a function of p_T^V a new physics model with a cut off $\Lambda = 1\ TeV$ [2]

Restoration of the Electroweak symmetry: At high energies, all SM particles become effectively massless and the longitudinal polarization are replaced back by the Goldstone Bosons.

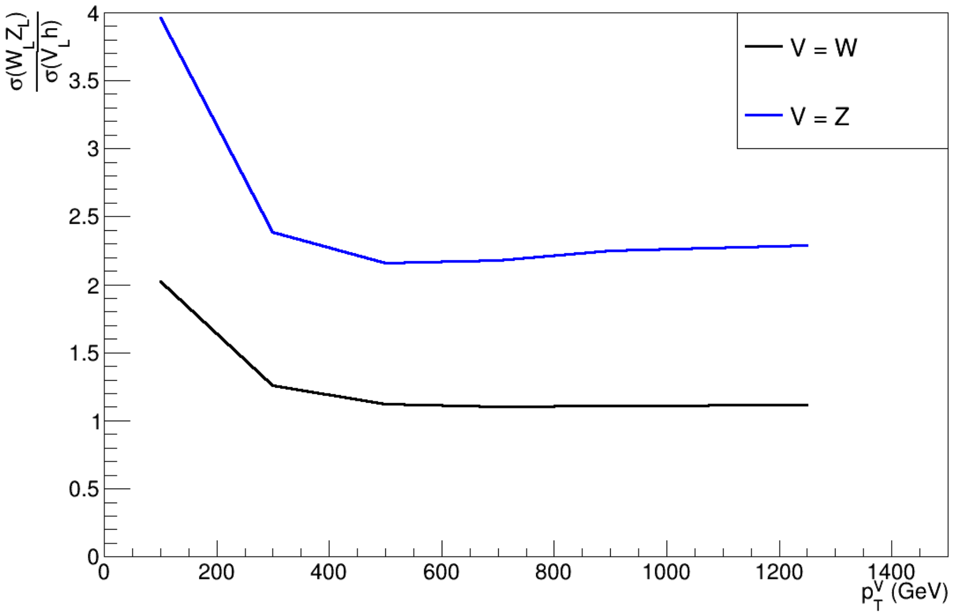

Important prediction of restoration of electroweak symmetries at high energies is

$\frac{\sigma(W_0Z_0)}{\sigma(W_0h)} \approx 1$ and $\frac{\sigma(W_0Z_0)}{\sigma(Z_0h)} \approx 2$ as shown in the figure below[2].

Ref [1]: R. Franceschini, G. Panico, A. Pomarol, F. Riva and A. Wulzer, JHEP 02 (2018) 111, Ref [2]: D. Liu and L.-T. Wang, Phys. Rev. D99 (2019) 055001

Radiation Amplitude Zero Effect

- The RAZ effect is expected for Wγ and WZ, not for WW or ZZ.
- $f_{00} \approx 20-30\%$ for WZ and $f_{00} \approx 5\%$ for WW at high p_T^W
- RAZ has been experimentally observed for Wγ[5][6] in D0 and CMS but no studies done for WZ production yet.

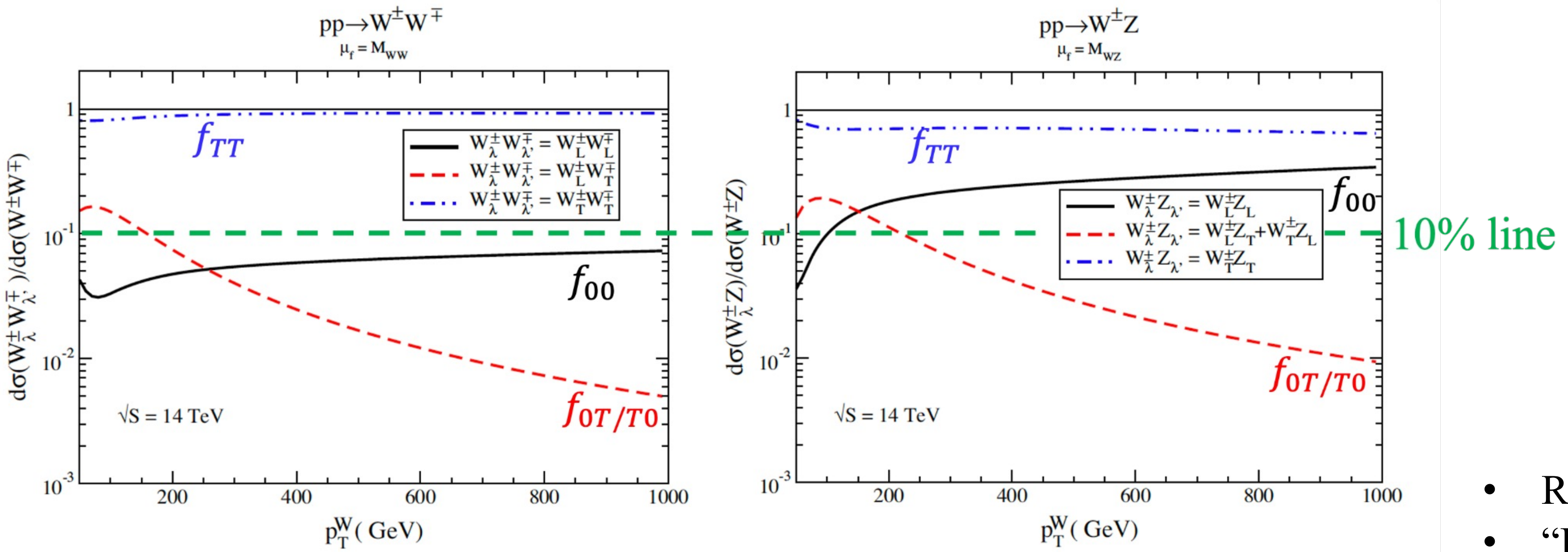

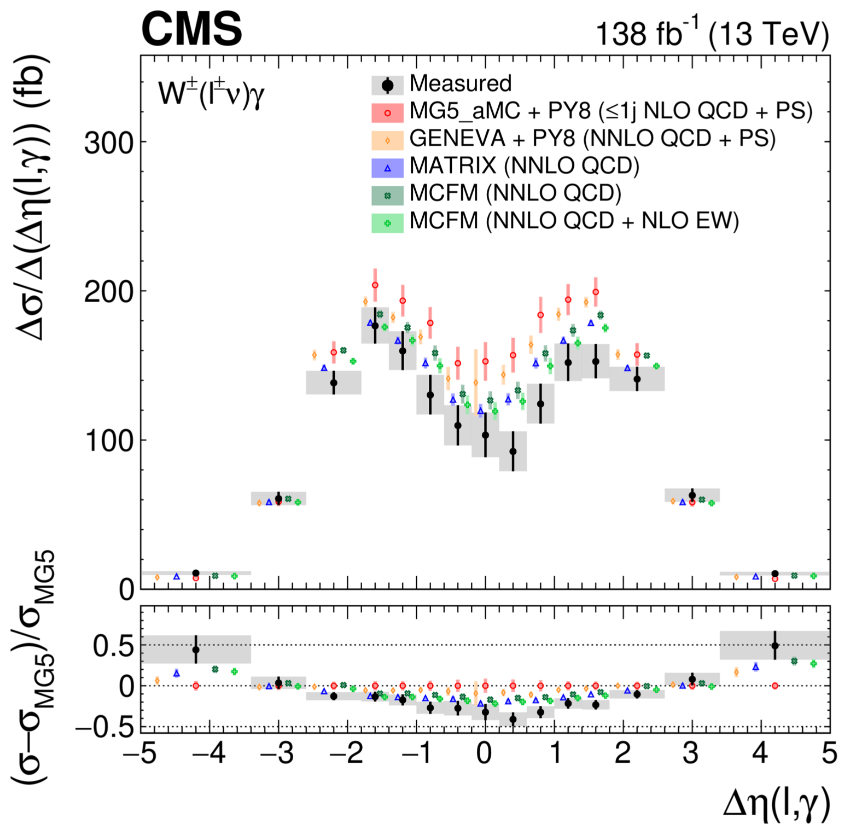

- RAZ effect observed at CMS for $W\gamma$ production.
- "Pronounced dip is observed" in the region of $\Delta\eta(\ell,\gamma)\sim 0$.[5]

- Expect to also observe pronounced dips near 0 for the $\Delta Y(W,Z)$ and $\Delta Y(\ell_W,Z)$ distributions
- However, experimentally challenging, and theorists were pessimistic that the RAZ effect can be observed in WZ events[3]

Ref [6]: L. Huang, S. D. Lane, I. M. Lewis and Z. Liu, Phys. Rev. D 103 (2021) 053007

Previous Diboson Polarization Measurement

- **Inclusive Fiducial phase space** for cross-section measurement and joint and single polarization fraction extraction
- Polarized samples are produced at LO with WZ+0,1 jets.
- Many validations are done to get NLO-accurate templates using LO polarized samples via DNNs.

Polarization State	Fractions of $W^{\pm}Z$	Significance: Observed (Expected)
f_{00}	0.067 ± 0.010	$7.1\,\sigma$ ($6.2\,\sigma$)
f_{0T}	0.110 ± 0.029	$3.4\,\sigma$ ($5.4\,\sigma$)
f_{T0}	0.179 ± 0.023	$7.1\,\sigma$ ($6.6\,\sigma$)
f_{TT}	0.644 ± 0.032	$11\,\sigma$ ($9.7\,\sigma$)

arXiv:2211.09435, submitted to PLB

	Signal Region	
	Pre-fit	Post-fit
WZ in τ	620 ± 60	630 ± 60
ZZ	1420 ± 120	1630 ± 50
$t\bar{t}+V$	870 ± 130	830 ± 120
Misid. leptons	1170 ± 230	1010 ± 220
Others	800 ± 90	790 ± 90
W_0Z_0	920 ± 40	1190 ± 160
W_0Z_T	2670 ± 50	1900 ± 500
$W_\mathrm{T}Z_0$	2670 ± 60	3100 ± 400
$W_\mathrm{T}Z_\mathrm{T}$	10200 ± 230	10900 ± 600
Total MC	21400 ± 600	21950 ± 170
Data	—	21936

Contributions to Signal and Background Processes Pre and Post Fit

Polarized Sample Generation

- **MadGraph Polarized Sample Generation:**
  - Using MadGraph version 2.7.0+, one can produce WZ events with Transverse (T) or Longitudinal (0) polarization specified. (Left or Right polarized vector bosons cannot be generated)
    - NLO QCD corrections are NOT implemented for polarized processes in MadGraph
    - **WZ with 0+1 jets events produced to emulate NLO**
    - The polarization definition depends on the frame (not Lorentz Invariant). WZ rest frame is used for this definition.

- **For the official samples:**
  - WZ decay to e, μ is considered. (Samples with at least one τ are also produced separately).
  - Different samples are produced for $p_T^Z \geq 150$ GeV and $p_T^Z < 150$ GeV to increase statistics for events with high p_T^Z.

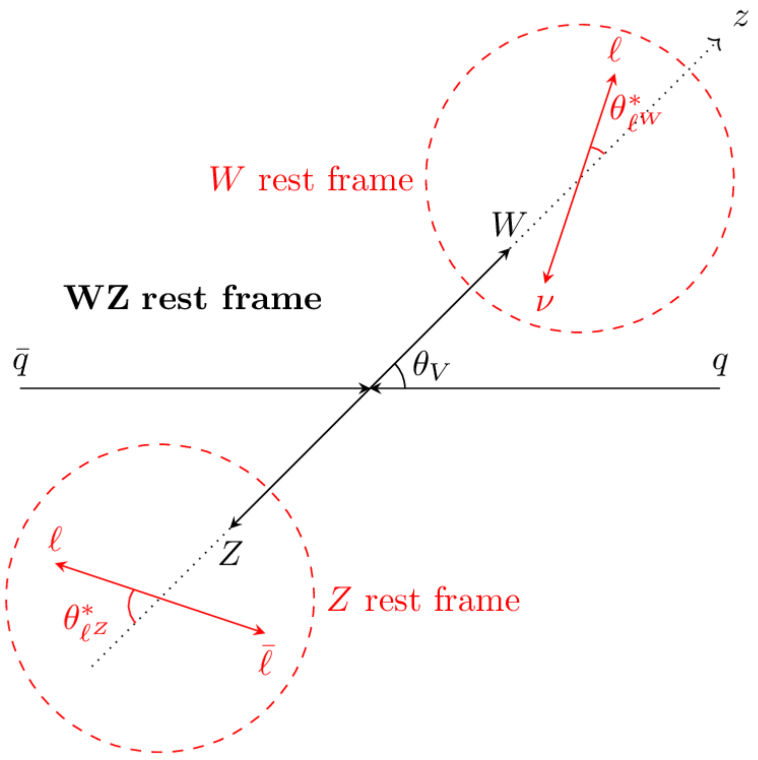

Variables defined in the modified helicity frame used for multivariate analysis

NLO QCD+EW Corrections:

$p_T^Z > 200$ GeV (00 fraction meas region)

- The MadGraph sample generation is done with LO with two processes (0 jet+1 jet) added together to emulate NLO effect more closely.
- The NLO QCD+EW calculations are added using theoretical calculations produced by theorists[6].

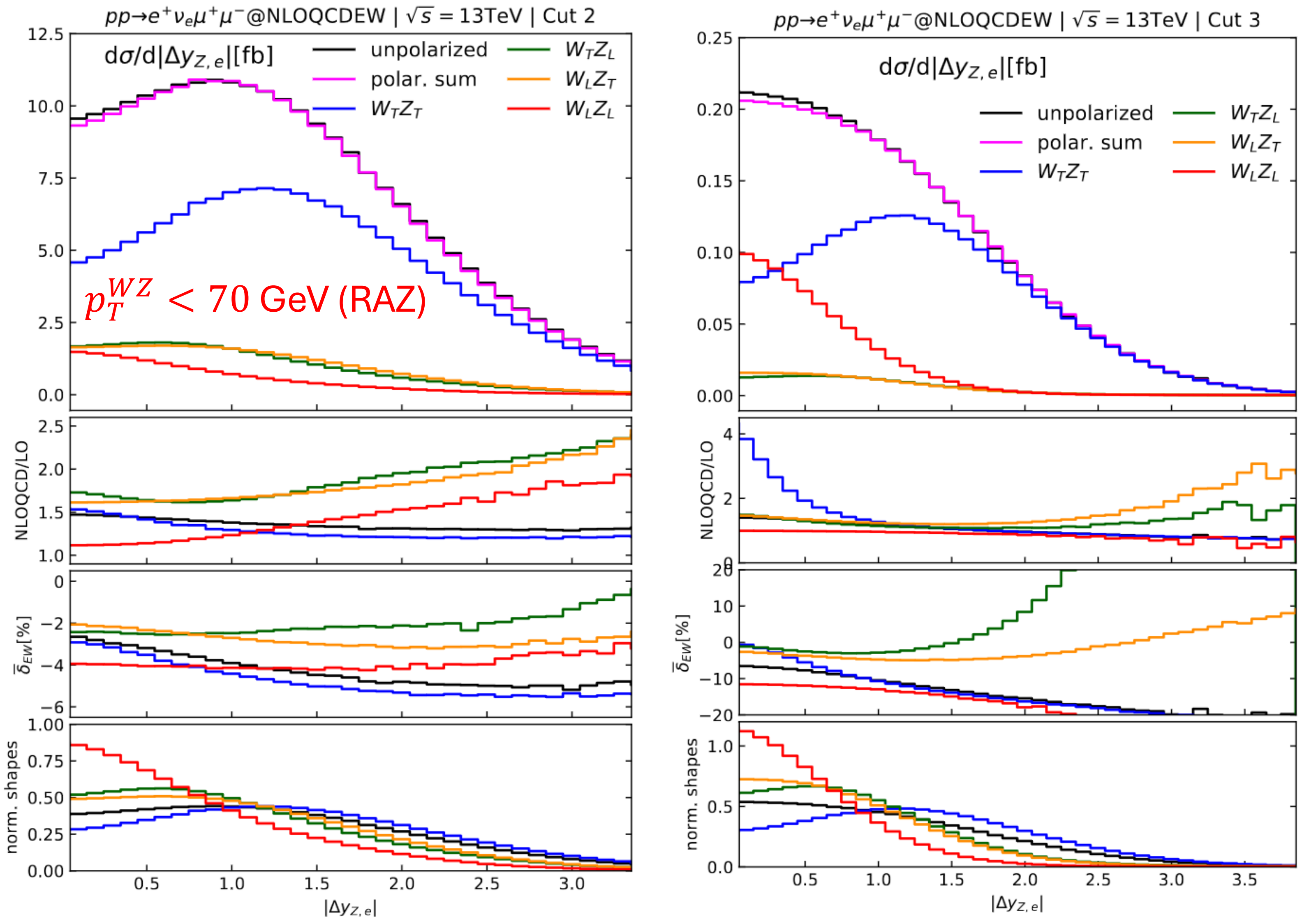

Ref [5]: Thi Nhung Dao, Duc Ninh Le "**Enhancing the doubly-longitudinal polarization in WZ production at the LHC**" arXiv:2302.03324 .

NLO QCD and EW Corrections

$$k_{factor} = \frac{MoCaNLO^{Parton}_{Polarized}}{MadGraph01LO^{Particle}_{Polarized}} \times \frac{Sherpa\_NLO^{Particle}_{Inclusive}}{MoCaNLO^{Parton}_{Inclusive}}$$

$$InterfNLO^{NLO} = \frac{MoCaNLO - \sum_{Pol} MoCaNLO_{Pol}}{MoCaNLO} \times Sherpa_N LO_{Incl} Reco$$

$$Reweighting factors = \frac{Inclusive - Interference}{PolarSum}$$

$$d_{\sigma_{NLO_+}} = d_{\sigma_{LO}} \times (1 + \delta_{QCD} + \delta_{EW})$$

$$\delta_{QCD} = \frac{d\Delta\sigma_{QCD}}{d\sigma_{LO}}, \delta_{EW} = \frac{d\Delta\sigma_{EW}}{d\sigma_{LO}}$$

$$d_{\sigma_{NLO_\times}} = d_{\sigma_{LO}} \times (1 + \delta_{QCD}) \times (1 + \delta_{EW})$$

Background Estimation

The background processes (we are not interested in) can mimic the signature of the signal processes.

- **The irreducible backgrounds** (with all prompt leptons) are estimated using the Monte Carlo simulation: $ZZ, VVV, WZ\ EW$ and $t\bar{t}V$
- **The reducible background** (mainly $t\bar{t}$ and $Z + jets$) with at least one fake lepton is estimated using a data-driven matrix method.
    - Fake rates calculated in bins of lepton p_T for electrons and muons.
    - Dedicated $Z + jets$ and $t\bar{t}$ contrW-associatedre used for Z and W associated leptons, this helps to account for the different fake composition
    - Good agreement between data and simulation in the inclusive region after fake background calculation
    - More relevant for the RAZ regions

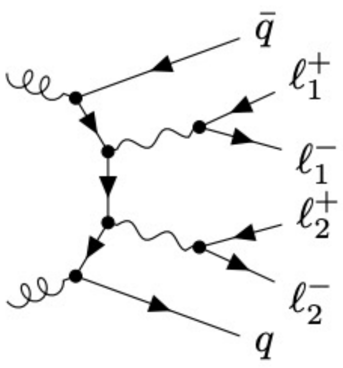

ZZ

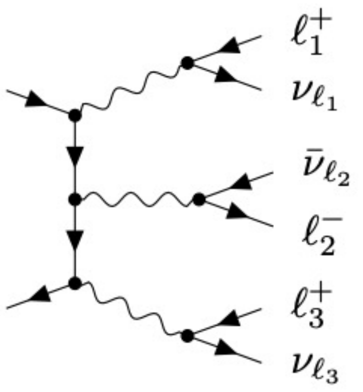

VVV

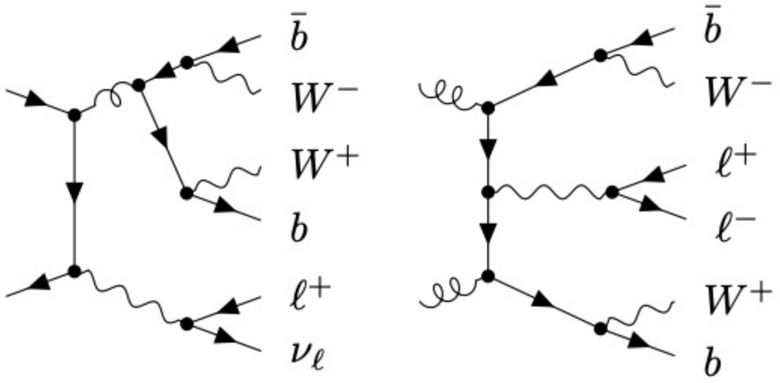

$t\bar{t}V$

Measurement of Radiation Amplitude Zero

Using Rapidity Difference between lepton of W and Z: $\Delta Y(W, Z)$

Data-bkg(including 00 0T T0) giving TT contributions compared with the MC.

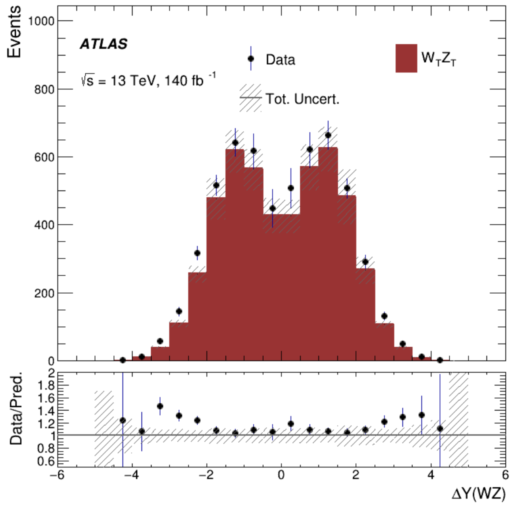

$p_T^{WZ} < 20$ GeV

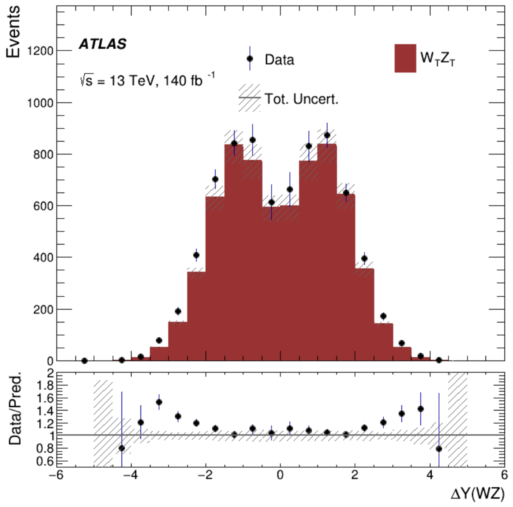

$p_T^{WZ} < 40$ GeV

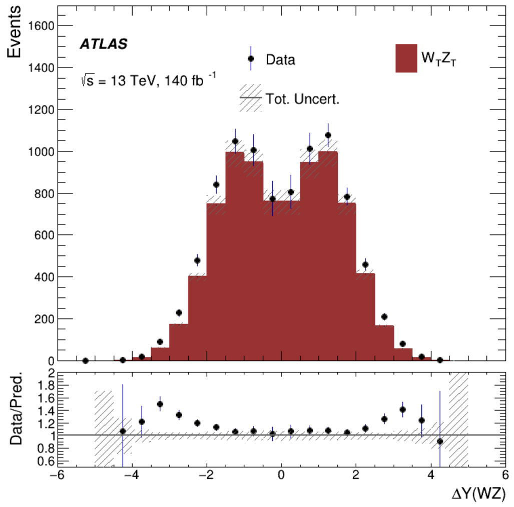

$p_T^{WZ} < 70$ GeV

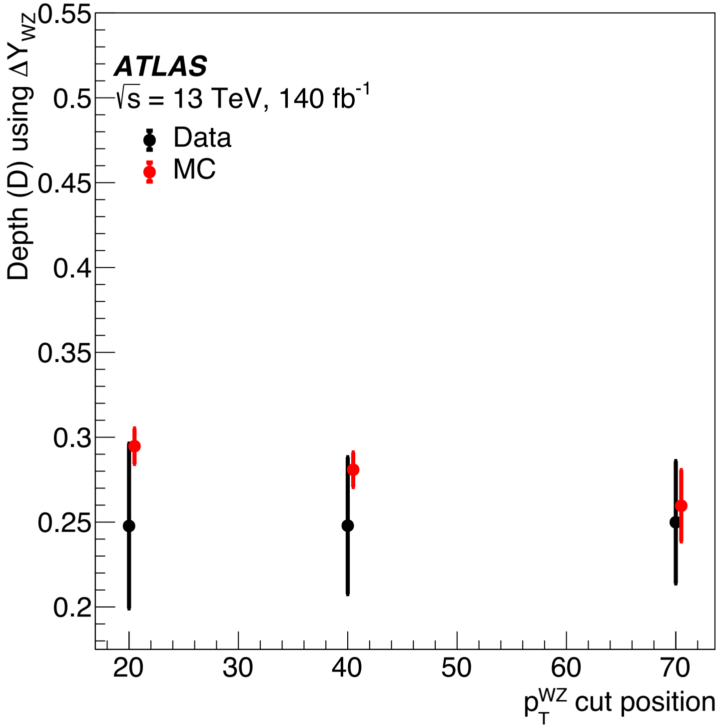

Unfolded Distributions

Unfolding of $\Delta Y(W, Z)$ Distributions

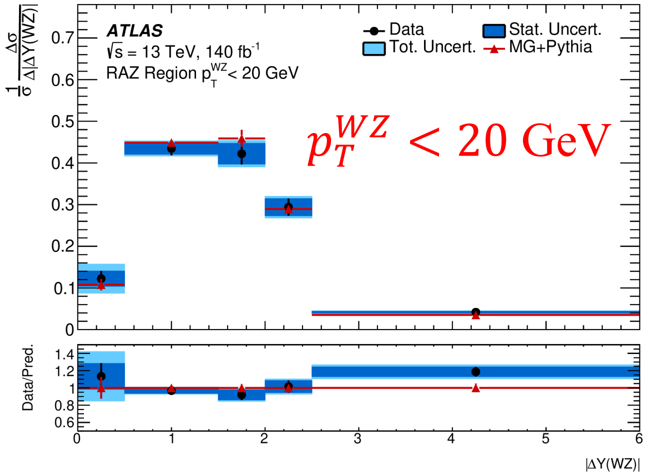

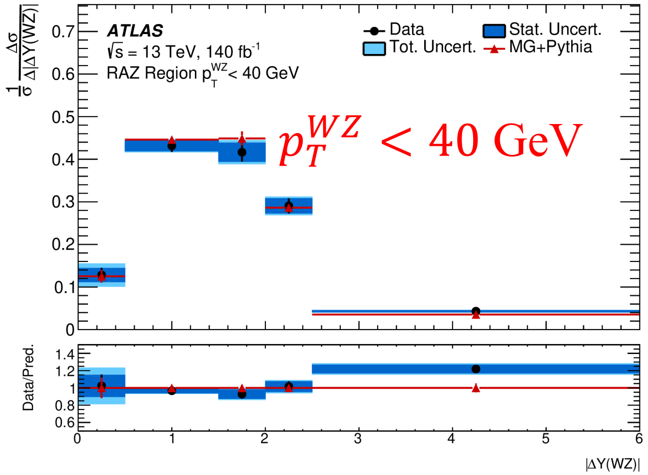

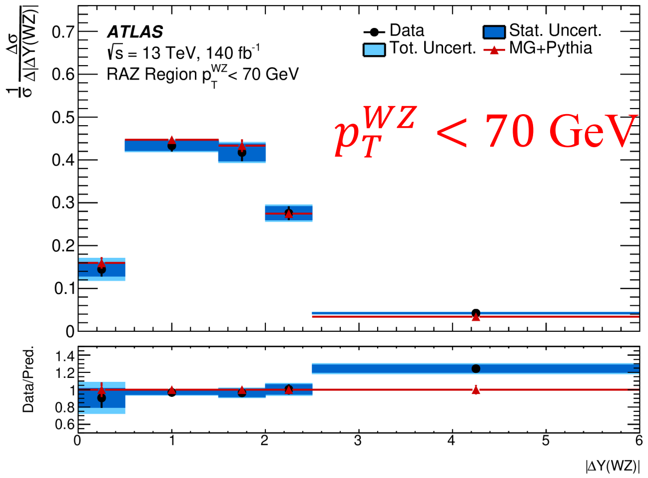

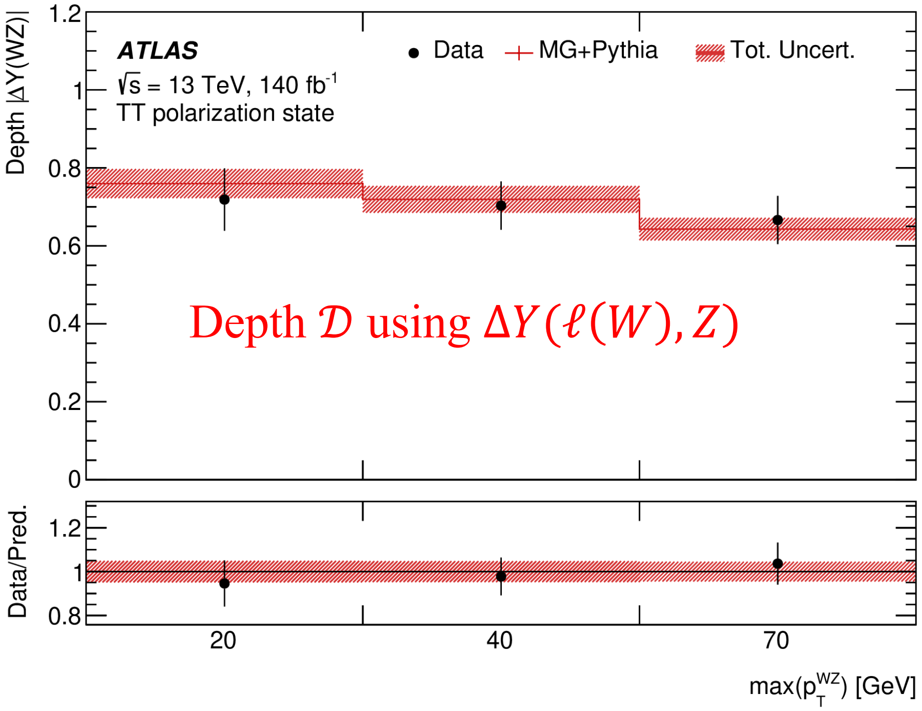

Event Selection and Trigger

Inclusive WZ event selection	
Event cleaning	Reject LAr, Tile and SCT corrupted events and incomplete events
Primary vertex	Hard scattering vertex with at least two tracks
Triggers in 2015	`HLT_e24_lhmedium_L1EM20VH || HLT_e60_lhmedium || HLT_e120_lhloose` `HLT_mu20_iloose_L1MU15 || HLT_mu50`
Triggers in 2016–2018	`HLT_e26_lhtight_nod0_ivarloose || HLT_e60_lhmedium_nod0 || HLT_e140_lhloose_nod0` `HLT_mu26_ivarmedium || HLT_mu50`
ZZ veto	Less than 4 baseline leptons
N leptons	Exactly three leptons passing the Z lepton selection
Leading lepton p_{T}	$p_{\mathrm{T}}^{\mathrm{lead}} > 25$ GeV (in 2015) or $p_{\mathrm{T}}^{\mathrm{lead}} > 27$ GeV (in 2016-2018)
Z leptons	Two same flavor oppositely charged leptons passing the Z-lepton selection
Z lepton invariant mass	$\|m_{\ell\ell} - M_Z\| < 10$ GeV
W lepton	Remaining lepton passes the W-lepton selection
W transverse mass	$m_{\mathrm{T}}^{W} > 30$ GeV
ΔR	$\Delta R(\ell_Z^-, \ell_Z^+) > 0.2$, $\Delta R(\ell_Z, \ell_W) > 0.3$

Signal regions			
	Radiation Amplitude Zero	**00-enhanced region 1**	**00-enriched region 2**
Pass inclusive WZ event selection	✓	✓	✓
Transverse momentum of the Z boson (p_T^Z)	-	[100, 200] GeV	> 200 GeV
Transverse momentum of the WZ system (p_T^{WZ})	< 20, 40, 70 GeV	< 70 GeV	< 70 GeV

Data MC Comparisons RAZ regions: $\Delta Y(\ell_W, Z)$

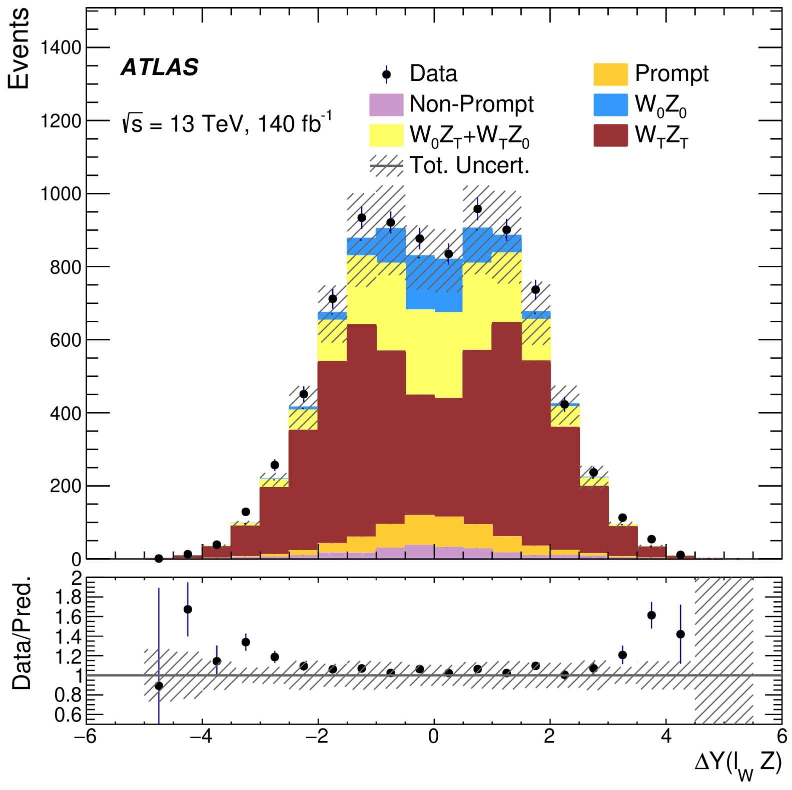

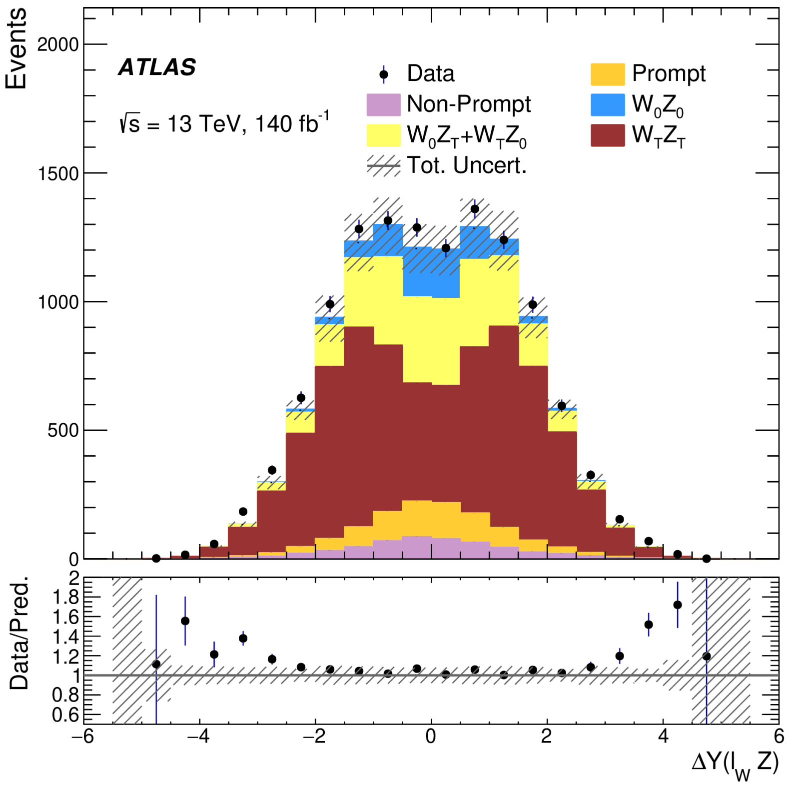

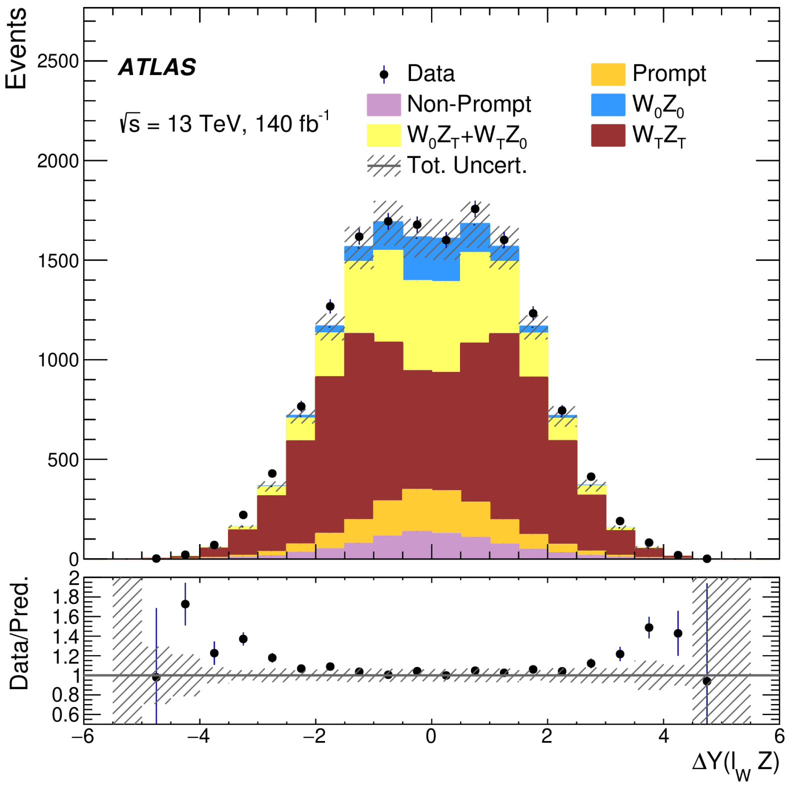

Data MC Comparisons RAZ regions: $\Delta Y(W,Z)$

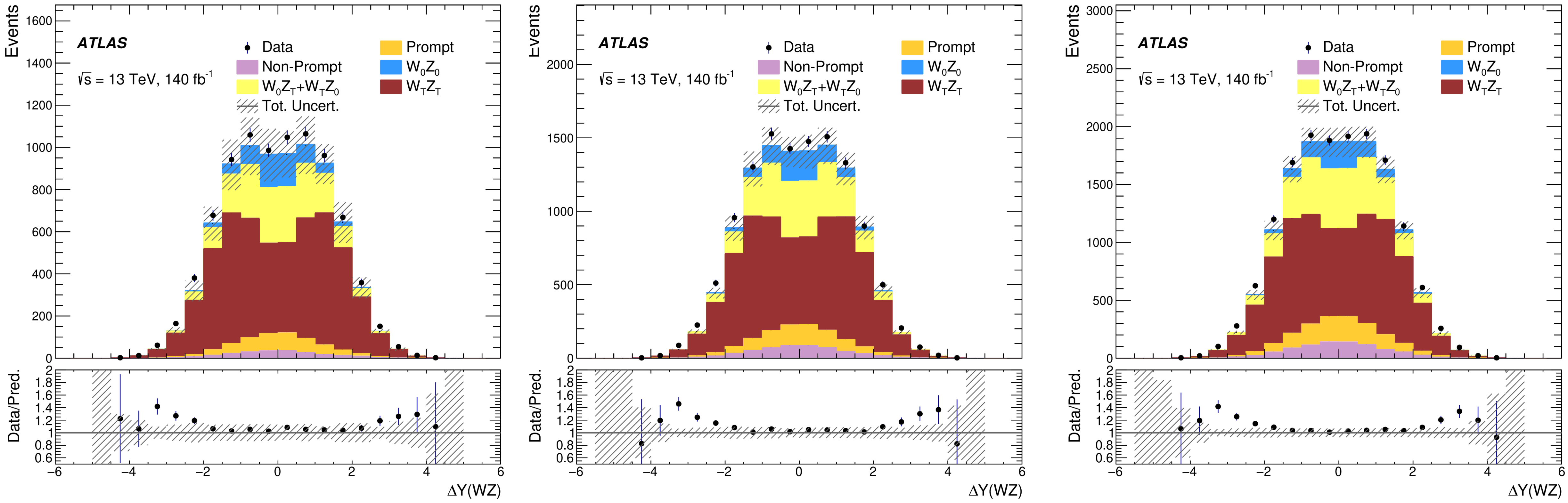

Unfolding Migration Matrices: $\Delta Y(\ell_W, Z)$

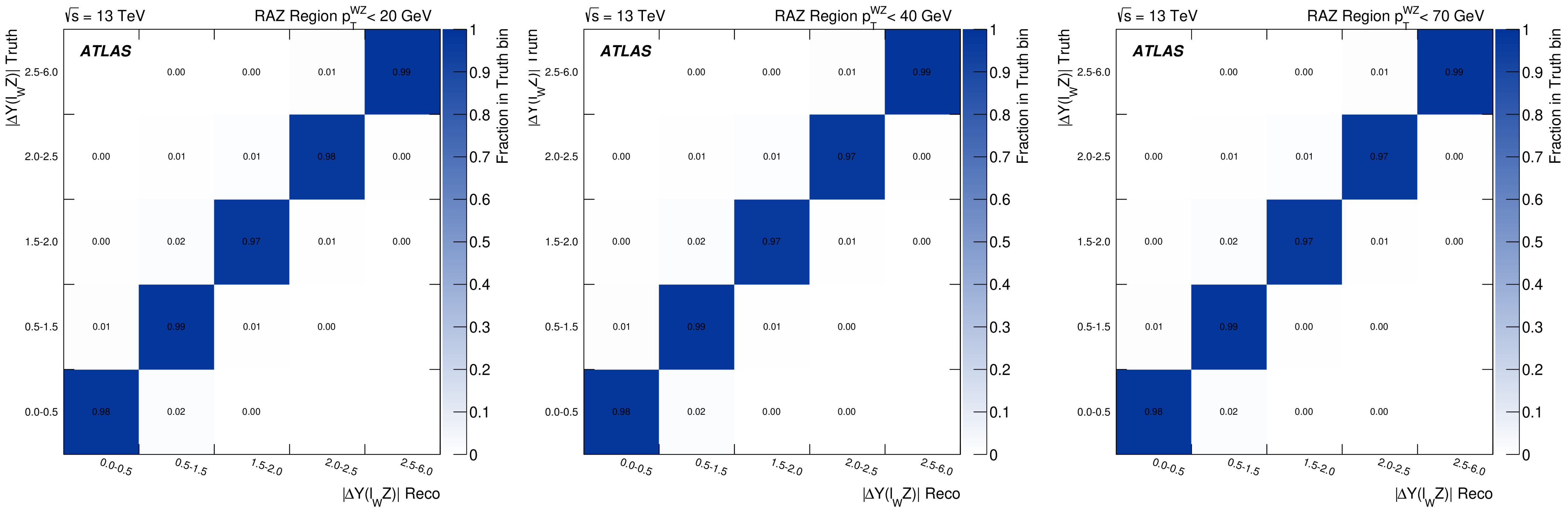

Unfolding Migration Matrices: $\Delta Y(W,Z)$

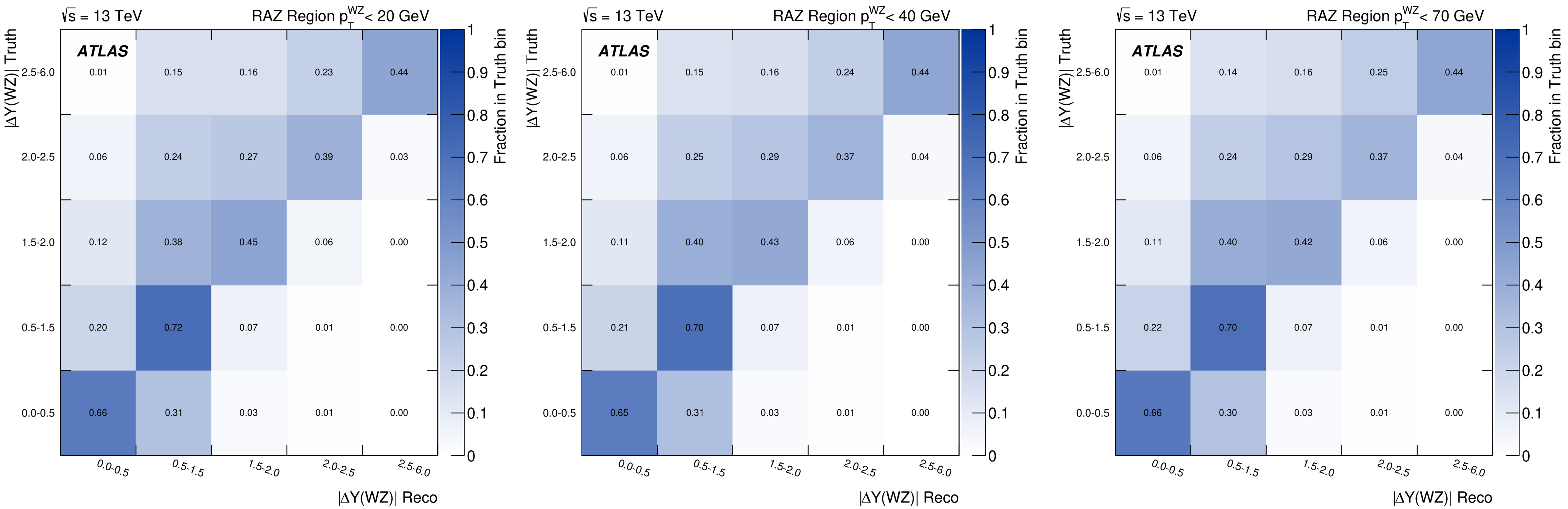

Uncertainties: $p_T^{WZ} < 20$ GeV

	Impact [%]			
Source	TT state		Sum of polarizations	
Experimental	$\Delta Y(\ell_W Z)$	$\Delta Y(WZ)$	$\Delta Y(\ell_W Z)$	$\Delta Y(WZ)$
Luminosity	1.2	0.5	0.3	0.1
Electron calibration	1.3	0.7	0.7	0.2
Muon calibration	1.9	0.7	1.1	0.8
Jet energy scale and resolution	8.1	3.6	2.0	1.0
$E_{\mathrm{T}}^{\mathrm{miss}}$ scale and resolution	0.3	0.8	0.4	1.0
Flavor-tagging inefficiency	0.0	0.0	0.0	0.0
Pileup modelling	1.3	1.3	2.7	0.4
Non-prompt background estimation	4.2	1.4	5.7	1.7
Modelling				
Background, other	4.0	1.4	4.9	1.5
Model statistical	2.3	1.3	4.1	2.2
NLO corrections	13.3	3.5	0.0	0.0
PDF, Scale and shower settings	13.1	5.4	0.7	0.5
Unfolding uncertainty	0.0	4.4	0.0	0.8
Experimental and modelling	21.5	9.1	9.3	3.7
Data statistical	13.3	6.5	24.1	11.7
Total	25.3	11.1	25.9	12.3

Uncertainties: $p_T^{WZ} < 40$ GeV

	Impact [%]			
Source	TT state		Sum of polarizations	
Experimental	$\Delta Y(\ell_W Z)$	$\Delta Y(WZ)$	$\Delta Y(\ell_W Z)$	$\Delta Y(WZ)$
Luminosity	1.4	0.5	0.4	0.1
Electron calibration	1.1	0.6	1.2	0.4
Muon calibration	1.9	0.8	1.1	0.6
Jet energy scale and resolution	5.1	2.5	1.2	1.1
E_T^{miss} scale and resolution	1.0	1.1	1.7	1.8
Flavor-tagging inefficiency	0.0	0.0	0.1	0.0
Pileup modelling	0.3	0.6	3.3	0.2
Non-prompt background estimation	7.2	2.5	10.0	2.7
Modelling				
Background, other	4.9	1.7	6.5	1.8
Model statistical	2.4	1.2	4.3	2.0
NLO corrections	11.3	1.7	0.0	0.0
PDF, Scale and shower settings	9.0	4.3	0.6	0.3
Unfolding uncertainty	0.0	1.4	0.0	0.9
Experimental and modelling	18.0	6.5	13.3	4.5
Data statistical	13.3	5.9	26.0	10.3
Total	22.4	8.8	29.2	11.2

Uncertainties: $p_T^{WZ} < 70$ GeV

	Impact [%]			
Source	TT state		Sum of polarizations	
Experimental	$\Delta Y(\ell_W Z)$	$\Delta Y(WZ)$	$\Delta Y(\ell_W Z)$	$\Delta Y(WZ)$
Luminosity	1.5	0.6	0.5	0.1
Electron calibration	0.9	0.5	1.7	0.4
Muon calibration	1.6	0.8	1.4	0.5
Jet energy scale and resolution	3.4	1.9	1.8	1.2
$E_{\mathrm{T}}^{\mathrm{miss}}$ scale and resolution	1.3	1.0	2.2	1.4
Flavor-tagging inefficiency	0.0	0.0	0.1	0.0
Pileup modelling	0.0	0.4	3.4	0.4
Non-prompt background estimation	9.5	3.6	13.5	3.7
Modelling				
Background, other	5.7	2.1	8.0	2.1
Model statistical	2.4	1.3	4.6	2.0
NLO corrections	9.2	1.0	0.0	0.0
PDF, Scale and shower settings	7.5	3.9	0.7	0.2
Unfolding uncertainty	0.0	2.3	0.0	2.6
Experimental and modelling	17.0	6.8	17.2	5.7
Data statistical	12.8	6.2	27.0	10.3
Total	21.3	9.3	32.0	11.8

Variable Definitions

Training variable	Definition
$\Delta Y(\ell_W Z)$	Rapidity difference between the W lepton and Z boson
p_T^{WZ}	Transverse momentum of the WZ system
$p_T(\ell_W)$	Transverse momentum of the W lepton
$p_T(\ell_2^Z)$	Transverse momentum of the subleading Z lepton
E_T^{miss}	Missing transverse momentum
$\cos\theta_{\ell_Z}$	Cosine of the angle of the Z lepton in the WZ rest frame w.r.t the z-axis
$\cos\theta_{\ell_W}$	Cosine of the angle of the W lepton in the WZ rest frame w.r.t. the z-axis

Yields in the high p_T^Z signal regions

Process	$100 < p_T^Z \leq 200$ GeV		$p_T^Z > 200$ GeV	
	Pre-fit	Post-fit	Pre-fit	Post-fit
W_0Z_0	222 ± 5	290 ± 60	47.6 ± 1.5	28 ± 19
$W_0Z_T + W_TZ_0$	323 ± 12	280 ± 140	23.7 ± 0.8	50 ± 40
W_TZ_T	856 ± 31	920 ± 100	124 ± 4	132 ± 29
Prompt background	169 ± 18	166 ± 18	24.1 ± 2.7	24.2 ± 2.7
Non-prompt background	68 ± 29	80 ± 40	2.8 ± 1.1	2.8 ± 1.1
Total Expected	1640 ± 60	1740 ± 40	222 ± 8	236 ± 15
Data	1740		236	

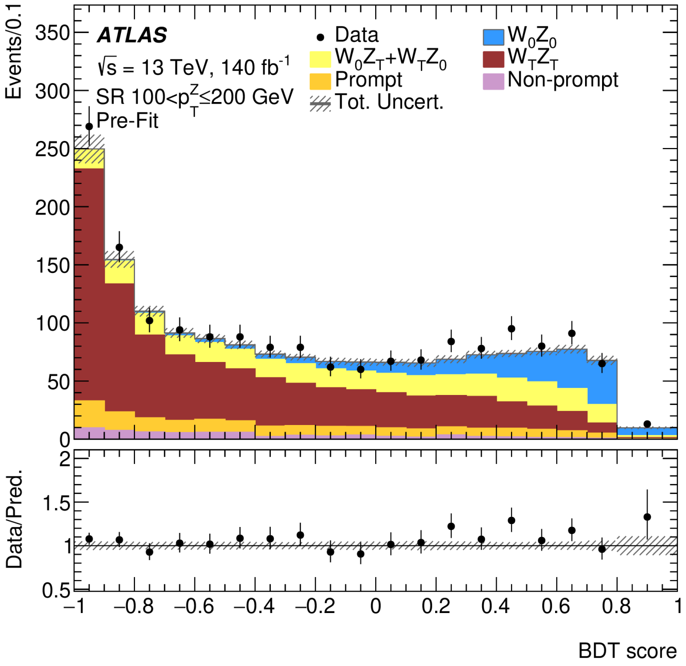
ATLAS
√s = 13 TeV, 140 fb-1
SR 100<p_T^Z≤200 GeV
Pre-Fit
Data
W0ZT+WTZ0
Prompt
Tot. Uncert.
W0Z0
WTZT
Non-prompt
Events/0.1
Data/Pred.
BDT score

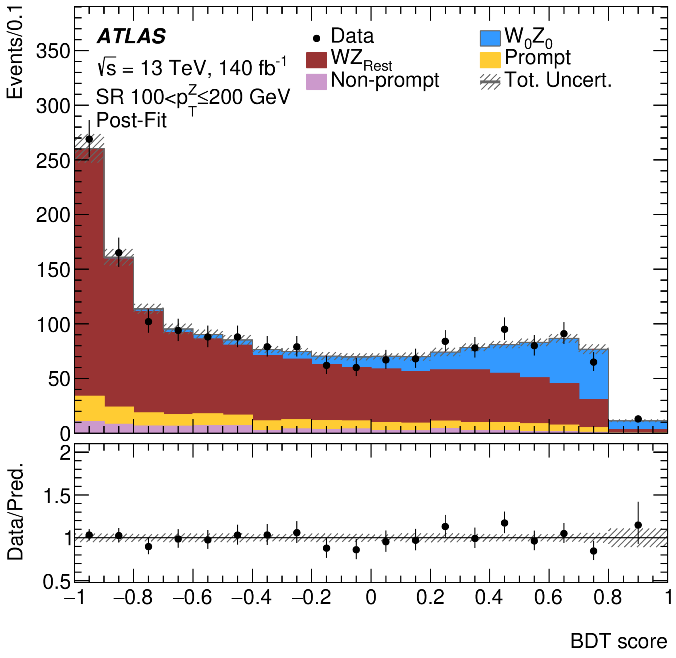
ATLAS
√s = 13 TeV, 140 fb-1
SR 100<p_T^Z≤200 GeV
Post-Fit
Data
WZRest
Non-prompt
W0Z0
Prompt
Tot. Uncert.
Events/0.1
Data/Pred.
BDT score

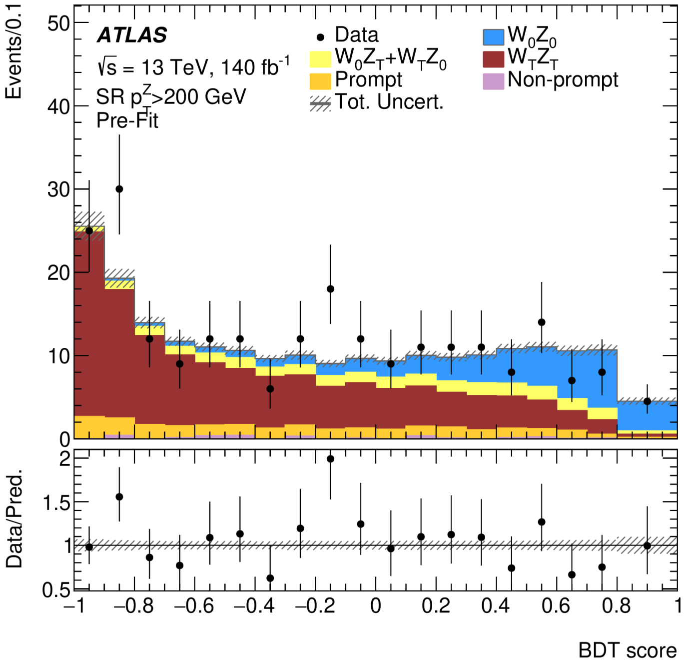
ATLAS
√s = 13 TeV, 140 fb-1
SR p_T^Z>200 GeV
Pre-Fit
Data
W0ZT+WTZ0
Prompt
Tot. Uncert.
W0Z0
WTZT
Non-prompt
Events/0.1
Data/Pred.
BDT score

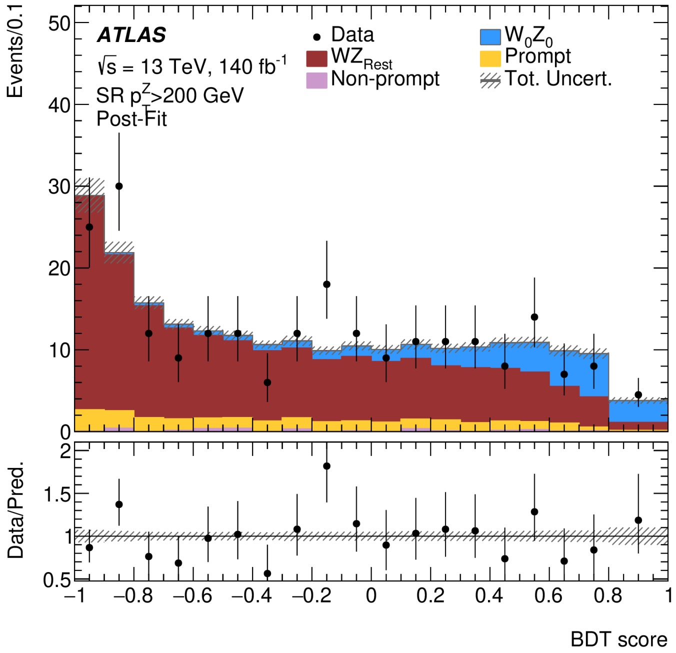
ATLAS
√s = 13 TeV, 140 fb-1
SR p_T^Z>200 GeV
Post-Fit
Data
WZRest
Non-prompt
W0Z0
Prompt
Tot. Uncert.
Events/0.1
Data/Pred.
BDT score

00 Fraction Measurement Uncertainties

Source	Impact on f_{00} [%]	
Experimental	**$100 < p_T^Z \leq 200$ GeV**	**$p_T^Z > 200$ GeV**
Luminosity	0.1	0.1
Electron calibration	1.0	0.9
Muon calibration	0.6	0.6
Jet energy scale and resolution	3.1	4.8
E_T^{miss} scale and resolution	0.3	0.3
Flavor-tagging inefficiency	0.0	0.0
Pileup modelling	1.0	0.7
Non-prompt background estimation	3.6	0.6
Modelling		
Background, other	0.9	0.9
Model statistical	1.6	2.2
NLO QCD effects	3.7	9.1
NLO EW effects	0.9	7.5
Effect of additive vs multiplicative QCD+EW combination	0.5	1.7
Interference impact	2.4	1.4
PDF, Scales, and shower settings	4.0	4.0
Experimental and modelling	8.1	13.9
Data statistical	11.4	31.4
Total	14.0	34.4